Jones, M.M., Sageman, B.B., Selby, D., Jicha, B.R., Singer, B.S., and Titus, A.L., 2020, Regional chronostratigraphic synthesis of the Cenomanian-Turonian Oceanic Anoxic Event 2 (OAE2) interval, Western Interior Basin (USA): New Re-Os chemostratigraphy and $^{40}Ar/^{39}Ar$ geochronology: GSA Bulletin, https://doi.org/10.1130/B35594.1.

Supplemental Material

$^{40}Ar/^{39}Ar$ Geochronology

Single crystal incremental heating experiments were performed on sanidine from samples NC-B, -C, and –D. Rank order plots of these results are shown in Fig. S1. Single crystal total fusion experiments were performed on samples K-07-01C and 90-O-34 (Fig. S2). Complete Ar isotope data for all experiments are provided in Tables S4 and S5.

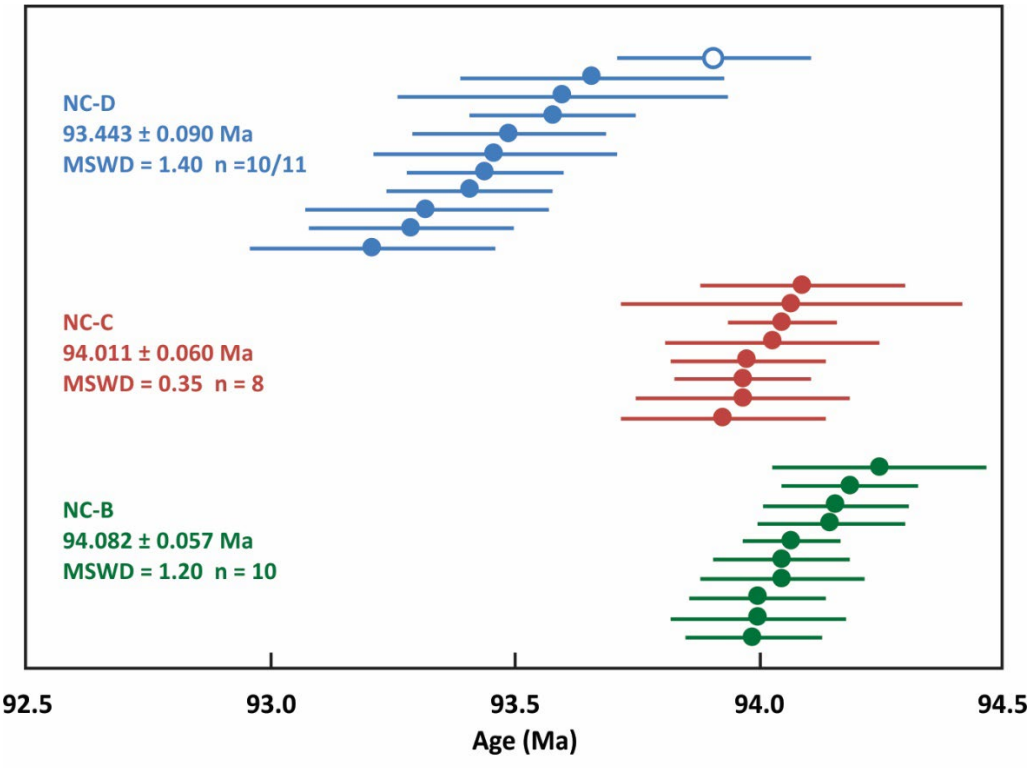

Figure S1. Rank order plot showing single sanidine $^{40}Ar/^{39}Ar$ plateau ages for NC-B (green), NC-C (red), and NC-D (blue) bentonites. Individual plateau and weighted mean ages are shown with 2σ uncertainties that include J uncertainty. White data points have been excluded from weighted mean calculations. For complete data see Table S4.

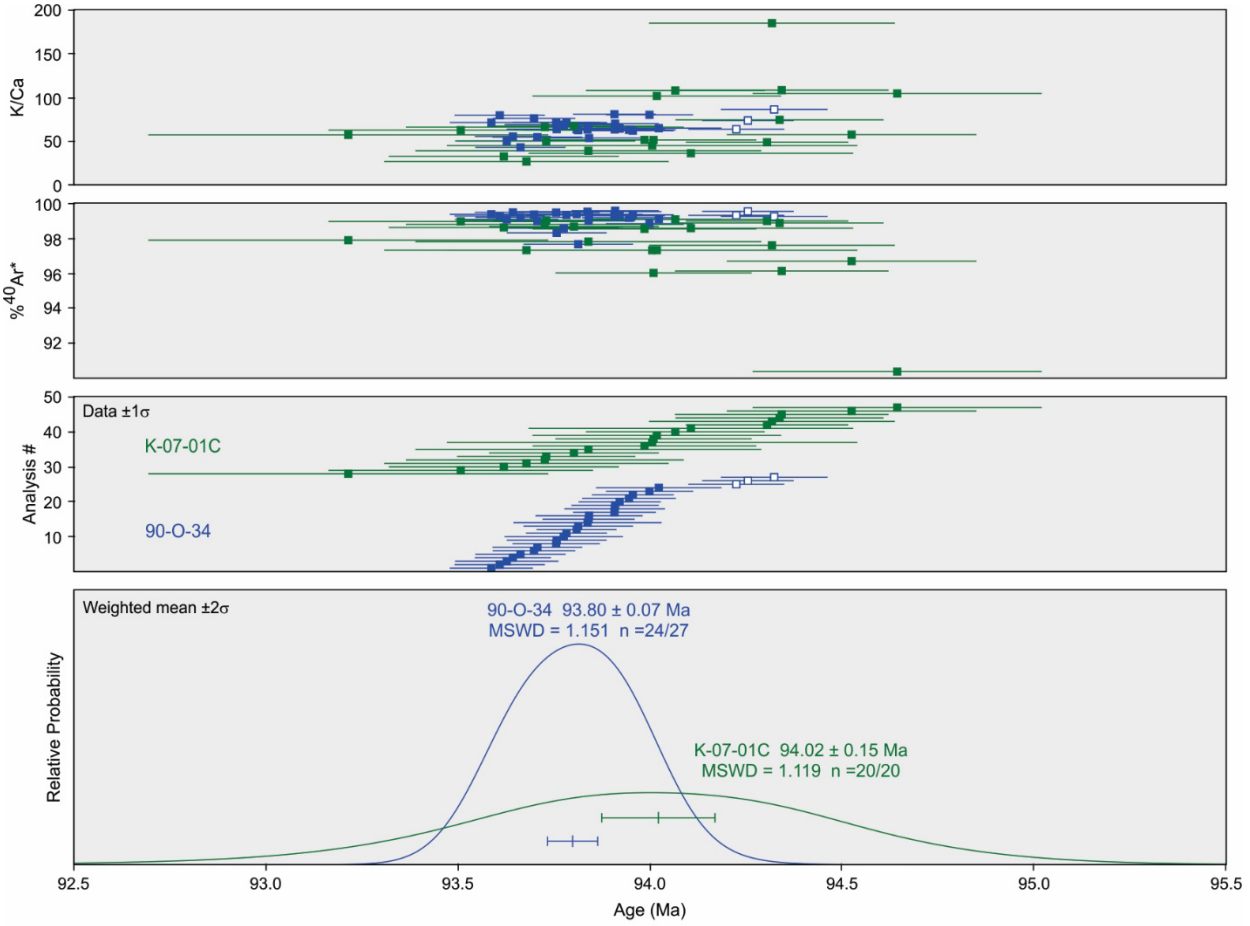

Figure S2. $^{40}Ar/^{39}Ar$ single crystal sanidine total fusion data for K-07-01C (green) and 90-O-34 (blue). Data shown as plots of A) K/Ca and B) % radiogenic ^{40}Ar ($\%^{40}Ar^*$) vs. Age (Ma), as well as C) rank order plots of each sample and D) probability density curves of each dataset. Dates are shown with 1σ analytical uncertainties. Weighted mean ages are show with 2σ uncertainties that include J uncertainty. White datapoints have been excluded from weighted mean calculations. For complete data see Table S5.

Nipple Creek section

"NC-D" 93.443 Ma ±0.09/0.17

"NC-C" 94.01 Ma ±0.06/0.15

"NC-B" 94.08 Ma ±0.06/0.15

pycnodonte bed

Wahweap Wash section

Section by R.M. Leckie and E.L. Leithold

TT5 at 46m

Tropic Shale Fm.

%Carbonate (Tibert et al., 2003)

KPS1-2

updated from Jones et al. (2019)

Turonian (part)

Cenomanian (part)

W. devonense

N. juddii

S. gracile

M. mosbyense

Naturita Fm.

1-3cm

Guembelitria sharp decline

-5? *Neobulimina dominance*

-4 *Gavelinella* acme

-3

-2 "*Heterohelix* shift"

-1

1-5: Extinction Horizons (Elder, 1989)

SH#1 Core

updated from Jones et al. (2019)

Depth (m)

Stage

Strat. Unit

Core Box

ATS (ka)

Turonian

Tropic Shale Fm.

Cenomanian

Naturita Fm.

M. chiastius

A. albianus

Bentonites

~600 km E

% TOC

% Carbonate

fs12*

fs11*

fs10*

thin local bent.

fs9*

fs8*

fs7*

fs6

fs5

fs4

fs3

fs2b

fs2a

fs0

OAE2

$\delta^{13}C_{org}$ (‰ VPDB)

Os_i

Portland Core

(near Pueblo, CO base Turonian GSSP)

Turonian

Cenomanian

Hartland

Bridge Creek Limestone

M. nodo.

V.b.

P.f.

W. devon.

N. juddii

S. gracile

84/LS7

79/LS6

LS5

77/LS4

73/LS3

67/LS2

63

LS1

OAE2 = 617 ± 58 ka

Short eccentricity bandpass

148 ka

286 ka

204 ka

$\delta^{13}C_{org}$ (‰VPDB)

Portland Core data redrafted from Meyers et al. (2012)

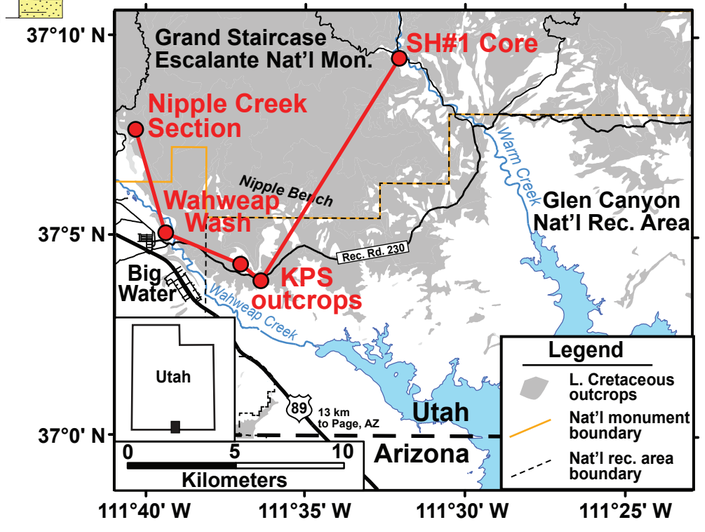

Kaiparowits Plateau Map

Lithologies

Marl, Coal, Mudstone, Sandstone, Calcareous shale, Bentonite, Sandy mudstone, Carbonate-rich bed, Shell-rich (outcrop), Muddy sandstone, Concretions, Heavy bioturbation

Equivalent scaling of depth at all sites except Portland Core

Figure S3. A stratigraphic correlation of four Cenomanian-Turonian boundary (CTB) interval sites along the Kaiparowits Plateau of southern Utah, USA (near Big Water) to the Portland Core near the base Turonian GSSP in Pueblo, Colorado, USA. For this study, three bentonite samples were measured from the Nipple Creek section for $^{40}Ar/^{39}Ar$ geochronology (Fig. S1 and Table S1) and an initial osmium isotope (Os_i) chemostratigraphy was measured for the SH#1 Core. Note the NC-D bentonite date is considered an outlier measurement in this study (see Discussion). The CTB interval bentonites A-D (Elder, 1988) are correlated regionally (red) along with flooding surfaces and limestone bed pairs in light blue (*sensu* Elder et al., 1994). Ammonite biostratigraphy and bentonite correlations for the KPS1-2 sections and the SH#1 Core are updated from Jones et al. (2019). The placements of bentonites C and D are now stratigraphically higher than in Jones et al. (2019) based on regional correlation and comparison of bentonite thicknesses at the Nipple Creek and Wahweap Wash sections. Carbonate content trends in Wahweap Wash section (Tibert et al., 2003) and in the SH#1 Core (Jones et al., 2019) also constrain correlations. Additionally, the CTB is now placed at 106.4m in the SH#1 Core based on this revised correlation to the KPS1-2 outcrop and bed 86 at the base Turonian GSSP (right). Ammonite subzones of *W. devonense* Biozone (i.e., *Pseudaspidoceras flexuosum – P.f.*, *Vascoceras birchbyi – V.b.*) are not plotted in KPS1-2. The Portland Core stratigraphic column and short eccentricity bandpass filter are re-drafted from Meyers et al. (2012) and $\delta^{13}C_{org}$ data is from Sageman et al. (2006). Bentonite correlation to the Portland core permits anchoring of the ATS, represented by red short-eccentricity bandpass filter, to radioisotopic ages so that the age of the Cenomanian-Turonian boundary and base of the Turonian Stage can be obtained.

Cenomanian-Turonian Boundary Age Estimates

We calculate ages for the Cenomanian-Turonian boundary (CTB) by anchoring the floating astronomical time scale (ATS) of the Portland Core (Meyers et al., 2001) to the various new and recently measured $^{40}Ar/^{39}Ar$ and U/Pb dates for bentonites B, C and D in the Western Interior Basin (Table S1). The base of the Turonian Stage is defined at the global boundary stratotype section and point (GSSP) at Rock Canyon Anticline in Pueblo, Colorado, USA by the first occurrence (F.O.) of ammonite *Watinoceras devonense* at the base of limestone Bed 86 (Kennedy et al., 2000; 2005). Bed labels at the GSSP section derive from the designations of Cobban and Scott (1972) and Elder and Kirkland (1985), and include the regional bentonites A, B, C, and D found in the CTB interval across much of the Western Interior Basin (Elder, 1988). The USGS no. 1 Portland Core, drilled 30 km NW of the GSSP, preserves bentonite beds and limestone-marlstone couplets that correlate to the GSSP section (Sageman et al., 2006) and to southern Utah (Fig. S3). The core has been studied in detail, for example, to measure carbon and initial osmium isotope chemostratigraphy, as well as to develop an ATS through the CTB interval (Meyers et al., 2001; Meyers and Sageman, 2004; Sageman et al., 2006; Du Vivier et al., 2014). As a result, it is possible to readily identify the CTB in the Portland Core and calculate its age by assigning dates to bentonite horizons in the Portland Core from recent radioisotopic measurements and then calculating durations to the CTB from the ATS.

For each estimate of the CTB age from individual bentonite dates, we combine all sources of uncertainty in quadrature, including full radioisotopic uncertainty, stratigraphic uncertainty from stage boundary placement and/or core sampling (<25 k.y.), and ATS uncertainty, which is approximated as ±1/4 the duration of the short eccentricity tuning cycle (Sageman et al., 2014). The aggregate age of the CTB is calculated from the weighted mean age of all individual CTB age estimates (Eqn. 1).

Eqn. 1: weighted mean age $= \frac{\sum_i^N \left(\frac{age_i}{\sigma_i^2}\right)}{\sum_i^N \left(\frac{1}{\sigma_i^2}\right)}$

Eqn. 2: two-sigma standard deviation of weighted mean age $= 2 \times \sqrt{\frac{1}{\sum_{i=1}^N \left(\frac{1}{\sigma_i^2}\right)}}$

where: σ = one-sigma full age uncertainty for a calculation of the CTB age from a given bentonite sample measurement (i)

The weighted mean age for the CTB was calculated in two different scenarios in this study. For the first scenario, only the four new bentonite $^{40}Ar/^{39}Ar$ ages from this study (NC-B, NC-C, K-07-01-C, 90-O-34), excluding outlier sample NC-D, were used to calculate the age of the CTB. For the second scenario, all recently measured $^{40}Ar/^{39}Ar$ and U/Pb dates of the A-D bentonites, which did not show evidence for inheritance or being an outlier, were included in a calculation of the CTB age (Table S1).

TABLE S1. CENOMANIAN-TURONIAN BOUNDARY GEOCHRONOLOGY SUMMARY

Jones et al. (2020)

all Ar/Ar ages calculated relative to FCs of 28.201 Ma

Bentonite dates used to calculate the Cenomanian-Turonian Boundary age in the Portland Core.

Bentonite (A-D)	Sample name	Study	Technique	Age (Ma)	Uncertainty Myr (2sigma)	Total uncertainty Myr (2sigma)	Astronomical duration (Myr) to CTB in Portland Core	CTB age estimate	2 sigma CTB age uncertainty (quadrature)	comments
B	average	Meyers et al. (2012)	Ar/Ar	94.100	0.140	0.270	-0.168	93.932	0.272	*Meyers et al. (2012) mean argon-argon age for Bentonite B*
B	NE-08-01	Meyers et al. (2012)	U/Pb	94.010	0.040	0.140	-0.168	93.842	0.144	
B	Bighorn River	Barker et al. (2011)	U/Pb	94.140	0.120	0.190	-0.168	93.972	0.193	*weighted mean of youngest 3 (might not include decay constant uncertainties)*
B	K-07–01B	Jicha et al. (2016)	Ar/Ar	93.990	0.070	0.160	-0.168	93.822	0.223	
B	90-O-19	Jicha et al. (2016)	Ar/Ar	93.980	0.070	0.160	-0.168	93.812	0.223	
B	NC-B	this study	Ar/Ar	94.082	0.057	0.150	-0.168	93.914	0.154	
C	average	Meyers et al. (2012)	Ar/Ar	93.790	0.120	0.260	0.118	93.908	0.262	*Meyers et al. (2012) mean argon-argon age for Bentonite C*
C	NC-C	this study	Ar/Ar	94.011	0.060	0.150	0.118	94.129	0.154	
C	K-07-01C	this study	Ar/Ar	94.022	0.147	0.204	0.118	94.140	0.223	
D	90-O-34	Meyers et al. (2012)	Ar/Ar	93.670	0.210	0.310	0.266	93.936	0.312	
D	B3	Eldrett et al. (2015)	U/Pb	93.670	0.037	0.120	0.266	93.936	0.125	*Youngest 4 of 6 zircons measured. Unclear if Bentonite D from central WIB is preserved in Maverick Basin based on mapping of bed by Elder (1988).*
D	90-O-34	this study	Ar/Ar	93.799	0.070	0.160	0.266	94.065	0.164	

Cenomanian-Turonian Boundary Age	
weighted mean age (Ma):	93.95
2 sigma weighted uncertainty (Ma):	0.05

	Bentonite D
weighted mean age (Ma):	93.72
2 sigma weighted uncertainty (Ma):	0.09

	Bentonite B
weighted mean age (Ma):	94.04
2 sigma weighted uncertainty (Ma):	0.07

	Bentonite C
weighted mean age (Ma):	93.97
2 sigma weighted uncertainty (Ma):	0.11

*Additional bentonite dates *not* used to calculate the Cenomanian-Turonian Boundary age due to concerns about zircon inheritance or outliers.*

Bentonite (A-D)	Sample name	Study	Technique	Age (Ma)	Uncertainty Myr (2sigma)	Total uncertainty Myr (2sigma)	Astronomical duration (Myr) to CTB in Portland Core	CTB age estimate	2 sigma CTB age uncertainty (quadrature)	comments
B	K-07–01B	Meyers et al. (2012)	U/Pb	94.44	0.07	0.15	-0.168	94.272	0.15	*inherited zircons? Does not obey stratigraphic superposition, ~400 k.y. older than*
B	Bighorn River	Barker et al. (2011)	U/Pb	94.29	0.13	0.2	-0.168	94.122	0.20	*NE-08-01. weighted mean of all 6 zircon analyses*
C	AZLP-08-04	Meyers et al. (2012)	U/Pb	94.37	0.04	0.14	0.118	94.488	0.14	*inherited zircons? Does not obey stratigraphic superposition*
D	AZLP-08-05	Meyers et al. (2012)	U/Pb	94.09	0.13	0.19	0.266	94.356	0.19	*inherited zircons? Does not obey stratigraphic superposition*
D	NC-D	this study	Ar/Ar	93.443	0.09	0.16	0.266	93.709	0.16	*apparent outlier*

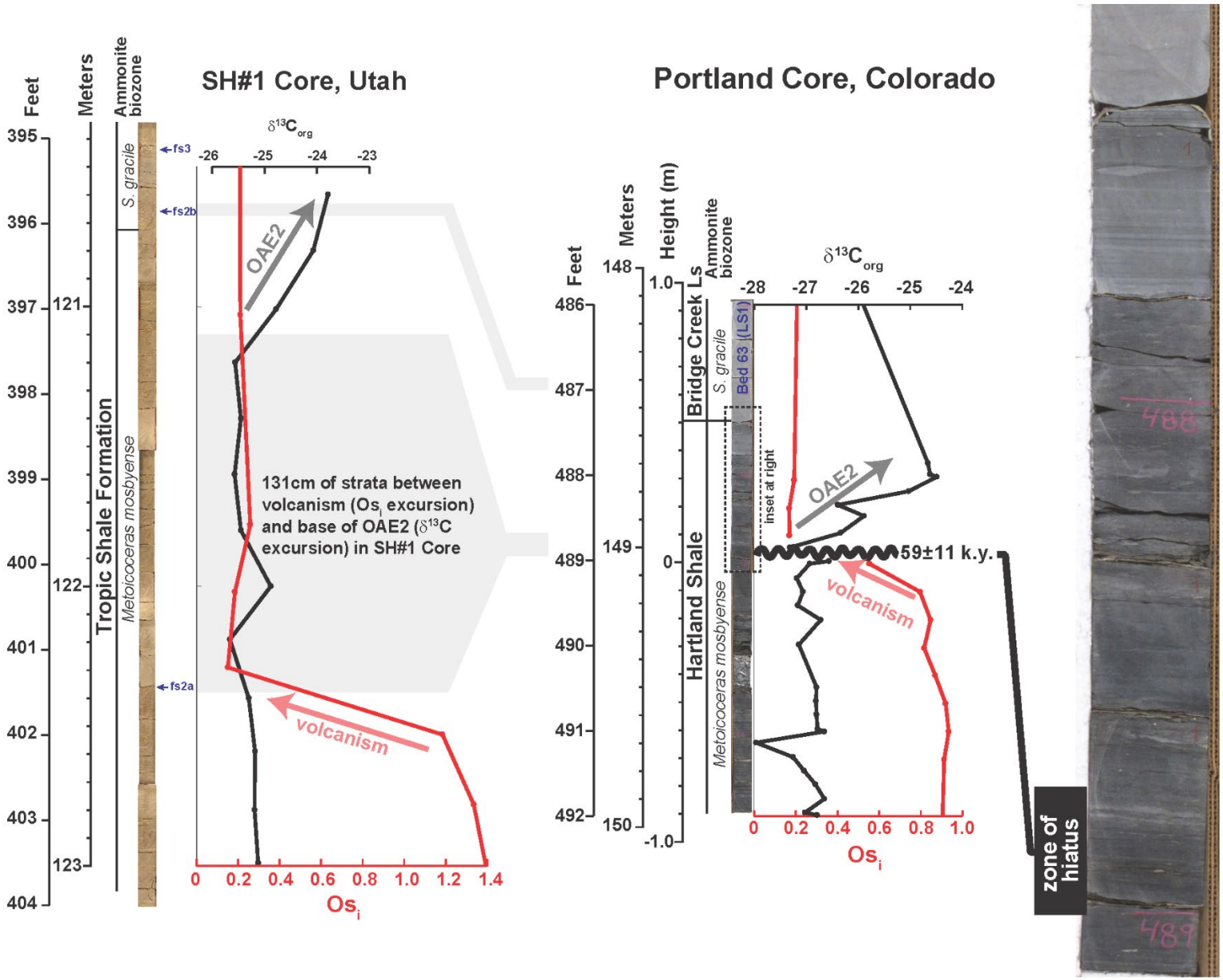
SH#1 Core, Utah
Feet
Meters
Ammonite biozone
Tropic Shale Formation
S. gracile
Metoicoceras mosbyense
fs3
fs2b
fs2a
δ13Corg
-26
-25
-24
-23
OAE2
131cm of strata between volcanism (Osi excursion) and base of OAE2 (δ13C excursion) in SH#1 Core
volcanism
0
0.2
0.4
0.6
0.8
1.0
1.2
1.4
Osi
395
396
397
398
399
400
401
402
403
404
121
122
123
Portland Core, Colorado
Feet
Meters
Height (m)
Ammonite biozone
Bridge Creek Ls
Hartland Shale
S. gracile
Metoicoceras mosbyense
Bed 63 (LS1)
inset at right
δ13Corg
-28
-27
-26
-25
-24
OAE2
59±11 k.y.
volcanism
zone of hiatus
0
0.2
0.4
0.6
0.8
1.0
Osi
486
487
488
489
490
491
492
148
149
150
1.0
0
-1.0

Figure S4. Core photos and chemostratigraphy of the OAE2 onset interval in the SH#1 (left) and Portland (right) cores. Note the expanded 131cm stratigraphic interval (grey shading) in SH#1 preserved between the initial osmium isotope (Os_i) excursion (this study - red) and the base of OAE2, which is defined by the characteristic positive $\delta^{13}C_{org}$ excursion (Jones et al., 2019). This interval is not preserved in the Portland Core of Colorado based on chemostratigraphic profiles (Os_i - Du Vivier et al., 2014; $\delta^{13}C_{org}$ - Sageman et al., 2006), a feature which is attributed to a hiatus. There is no readily visible lithological evidence for this hiatus in the uppermost Hartland Shale in the Portland Core to accompany the geochemical data (see inset at right). However, Pratt (1984) and Eicher and Diner (1989), quoted below, identified erosive and disconformable sedimentological features at a correlative stratigraphic horizon in the base Turonian GSSP section at Rock Canyon Anticline in Pueblo, Colorado (30 km SE of the Portland Core). It is unclear if this hiatus was generated directly by erosion from the relative sea level lowstand in the upper *Metoicoceras mosbyense* Ammonite Biozone or by the subsequent transgression. Strata in southern Utah preserve a >100km shoreline progradation in the upper *M. mosbyense* zone (Fig. 2) in the S1 genetic sequence of Laurin et al. (2019), consistent with a lowstand interpretation for the hiatus. However, the hiatus was initially identified as a bone bed at Pueblo (Eicher and Diner, 1989), a type of lithofacies that is commonly deposited from sediment starvation during transgression in epeiric seaways (Brett, 1995). Therefore, the 0.5cm bone bed at Pueblo could alternatively represent a condensed bed of ~60 k.y. duration that correlates to transgression at flooding surface 2a (fs2a) in the SH#1 Core and overlying strata of the Unit 6B interval of Uličný (1999). The base of the unradiogenic Os_i excursion in the SH#1 Core occurs in sandy mudstones overlying a flooding surface "fs2a" (Fig. 4), consistent with a pre-OAE2 amalgamated lowstand and transgression, and potentially a brief hiatus at this site, too. However, any putative hiatus at SH#1 would need to be geologically brief (<<59±10 k.y.) given the preservation of 1.3 meters of strata between the Os_i and $\delta^{13}C$ excursions (Fig. 4), and given recent correlations to nearby paralic sections (Laurin et al., 2019). More generally and regardless of the precise depositional mechanism, we consider the hiatus to be associated with the pre-OAE2 shoreline progradation and retrogradation pattern documented in the WIB (genetic sequence "S1" of Laurin et al., 2019) and lowstands in other basins globally (see discussion). More photos of the Portland Core are available at: https://my.usgs.gov/crcwc/core/report/11834. *S. gracile – Sciponoceras gracile*.

Observations consistent with a hiatus in the highest marly shale bed of the Hartland Shale from Rock Canyon Anticline in Pueblo, Colorado include:

> "A thin wavy-bedded layer (0.5cm thick) composed of bone fragments, phosphatic pebbles, and quartz sand is scoured into the uppermost marly shale." -Pratt (1984, p. 1150)

> "A lamina of phosphatic bone and tooth fragments at the base of the 55-cm marlstone bed is inferred to be a lag deposit that marks a significant break in deposition." -Eicher and Diner (1989, p. 136)

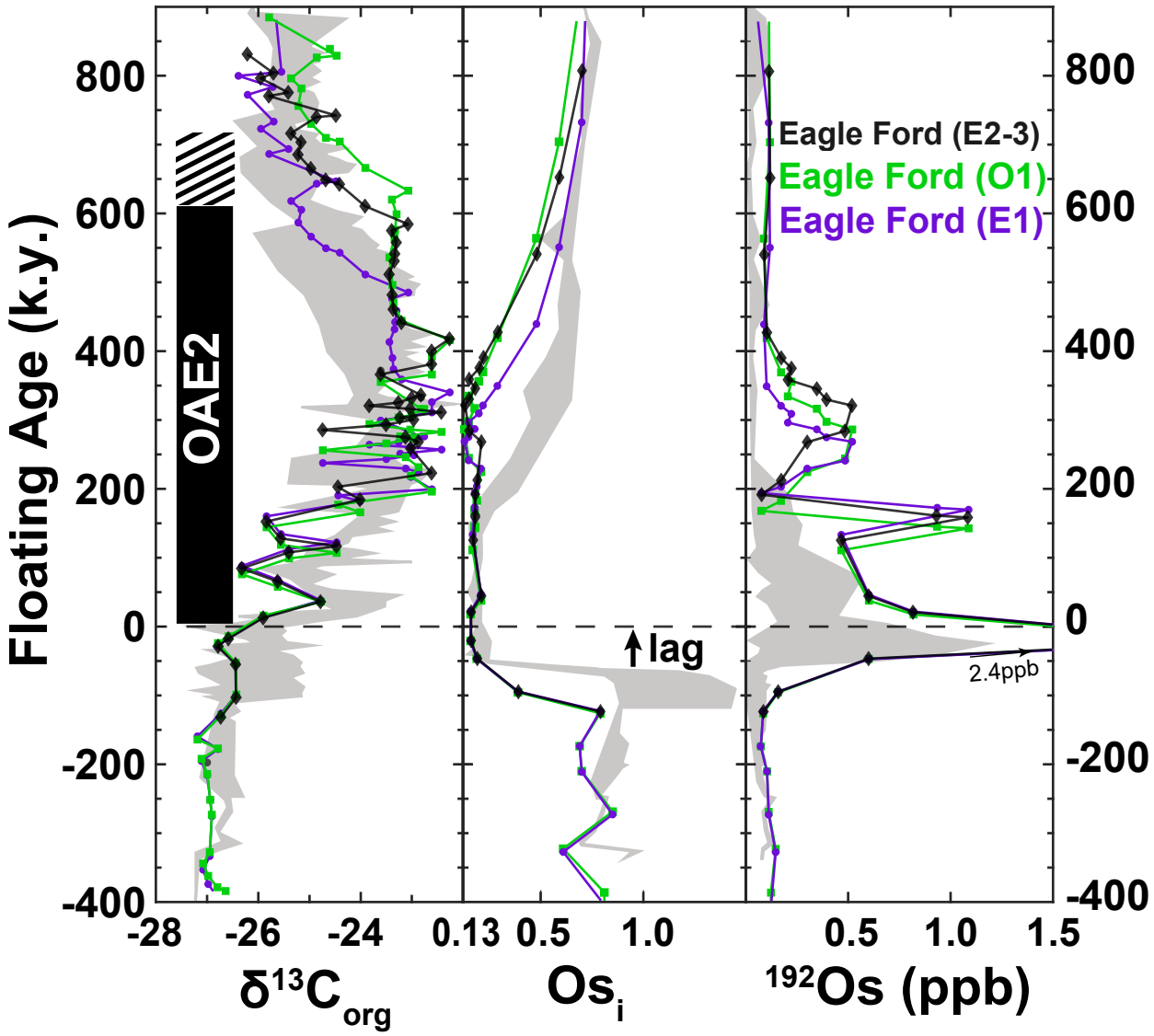

Figure S5. A comparison of floating astronomically-tuned geochemical timeseries spanning OAE2 from the mid-latitude sites of the Western Interior Basin (WIB, shaded records) with the Iona-1 Core of the Eagle Ford in Texas in the southernmost WIB (Meyers et al., 2001; Ma et al., 2014; Eldrett et al., 2015; Jones et al., 2019). From left to right - carbon isotopic ratios ($\delta^{13}C_{org}$) (Sageman et al., 2006; Joo and Sageman, 2014; Eldrett et al., 2015; Jones et al., 2019), initial osmium isotope ratios (Os_i) and ^{192}osmium concentrations (Du Vivier et al., 2014; Sullivan et al., 2020; this study). Different floating astronomical age models for the Eagle Ford data from long eccentricity bandpass (E1, purple circles) and obliquity tuning (O1, green square) scenarios (supplemental material of Eldrett et al., 2015) are plotted. A short eccentricity bandpass age model is also estimated (E2-3, black diamonds) from figure 9 of Eldrett et al. (2015). All records exhibit temporal lag between Os_i excursions and significant (>+1‰) $\delta^{13}C$ excursions defining the base of OAE2. Based on the $\delta^{13}C$ time series, the floating E1 age model of the Eagle Ford overlaps well with the age models from mid-latitude WIB sites, whereas the O1 age model indicates a longer duration of OAE2. Elevated ^{192}Os and unradiogenic Os_i values persist for 150-250 k.y. longer in the Eagle Ford than the WIB in each age model scenario during OAE2, potentially representing differences in circulation between regions or residual discrepancies in astronomical tuning among sites within the carbon isotope excursion interval.

Angus Core depth scale correction

Depths of samples horizons in the Angus Core were measured as centimeters offset from footage markers on slabbed core, for example 7474'-10cm (+cm = horizon deeper than foot marker, -cm = horizon shallower than foot marker). However, one of the footage markers (7475') in the Bridge Creek Limestone interval of the Angus Core was mismarked during original splitting of the core prior to donation to Northwestern University. Thus, samples with measured depths that reference this footage marker are offset from true depth. The corrections are as follows:

- <7475 feet - no corrections needed
- ≥7475 feet - add 19.92 cm to marked depth

Table S3 also corrected for core labeling and unit conversion. Although these depth offsets are relatively minor, it is necessary to correct for high-resolution evaluations of timing of the OAE2 chemostratigraphic record (one precession cycle ≈ 30-40 cm). It is also needed to ensure proper alignment of previous continuous XRF core scanning data, the foundation of the Angus core astronomical time scale (Ma et al., 2014), with discrete geochemical samples analyzed for $\delta^{13}C$ and Re-Os geochemical data (this study). Thus, depths of all legacy $\delta^{13}C_{org}$ data (Joo and Sageman, 2014) and new Re-Os data (this study) from the Angus Core are corrected prior to conversion to metric depths and plotting (Fig. 3; Tables 1, S2, S3).

TABLE S2. NEW WEIGHT PERCENT TOTAL ORGANIC CARBON (%TOC) AND CARBONATE CONTENT (%$CaCO_3$) FROM THE ANGUS CORE SPANNING THE ONSET OF OCEANIC ANOXIC EVENT 2.

ID	Updated Depth (m)	%CaCO3	%TOC
AA-18	2277.70	81.19	0.41
AA-18	2278.10	71.23	0.50
AA-18	2278.20	25.88	1.12
AA-18	2278.30	36.50	2.35
AA-18	2278.52	70.49	0.50
AA-18	2278.60	54.03	1.22
AA-18	2278.70	64.93	0.65
AA-18	2278.80	62.71	0.57
AA-18	2279.00	51.65	3.26
AA-18	2279.10	64.81	1.69
AA-18	2279.20	60.10	0.90
AA-18	2279.30	37.30	2.67
AA-18	2280.50	40.01	2.70
AA-18	2280.80	45.48	2.28
AA-18	2281.00	34.83	2.49
AA-18	2281.80	32.65	2.44
AA-18	2282.20	42.95	2.43
AA-18	2282.60	26.99	2.57

TABLE S3. CORRECTED ANGUS CORE DEPTHS OAE2 INTERVAL. GEOCHEMICAL DATA AND ORIGINAL DEPTHS FROM JOO & SAGEMAN (2014). IC%=INORGANIC CARBON (WT.%), OC% = ORGANIC CARBON (WT.%).

Originally published depth (m)	Depth(m) adjusted for core marking discrepancies	$\delta^{13}C_{org}$ (‰)	IC%	OC% (CaCO3 free)
2267.01	2268.03	-26.43	7.34	4.87
2267.51	2268.53	-26.01	8.73	2.21
2268.01	2269.02	-25.96	9.15	2.69
2269.05	2269.98	-25.75	4.32	2.08
2269.55	2270.52	-25.16	8.69	2.68
2270.05	2271.02	-24.88	7.52	3.65
2270.51	2271.48	-25.62	8.35	1.08
2271.01	2271.98	-25.10	7.24	1.96
2271.51	2272.48	-24.80	6.73	1.5
2272.01	2272.98	-24.25	7.8	3.65
2272.51	2273.48	-24.01	7.89	1.79
2273.01	2273.97	-23.80	6.51	4.23
2273.51	2274.48	-23.37	7.1	2.94
2273.97	2274.95	-24.06	7.11	1.4
2274.47	2275.45	-24.13	7.19	1.79
2274.97	2275.95	-23.71	6.84	3.87
2275.47	2276.45	-23.96	4.86	1.45
2275.94	2276.92	-24.48	3.00	0.98
2276.47	2277.45	-24.54	6.12	1.41
2277.00	2277.98	-25.38	4.55	7.56
2277.50	2278.48	-24.84	8.2	1.12
2278.00	2278.93	-25.48	6.7	2.61
2278.49	2279.42	-26.50	5.28	4.11
2278.54	2279.47	-26.23	5.23	3.61
2278.64	2279.57	-26.07	5.17	3.01
2278.69	2279.62	-26.73	4.27	4.69
2278.74	2279.67	-26.80	3.98	4.78
2278.79	2279.72	-26.39	4.5	4.45
2278.84	2279.77	-26.98	5.63	3.09
2278.94	2279.87	-26.56	6.78	1.87
2278.99	2279.92	-26.36	4.73	2.42
2279.04	2279.97	-26.66	3.93	4.08
2279.09	2280.02	-26.41	2.76	2.7
2279.14	2280.07	-26.14	3.16	3.4
2279.24	2280.17	-26.46	4.26	3.67
2279.29	2280.22	-26.45	4.53	3.77
2279.34	2280.27	-26.78	4.39	3.75
2279.39	2280.32	-26.31	4.84	4.09
2280.49	2281.40	-26.82	4.76	4.67
2281.99	2282.89	-27.11	6.92	5.97
2282.49	2283.38	-26.67	5.08	4.64
2282.99	2283.89	-26.65	6.05	4.52

Table S4. Complete $^{40}Ar/^{39}Ar$ results

Single crystal incremental heating

Sample: **NC-B**
Material: **sanidine**

File	Laser Power (%)	$^{40}Ar \pm 2\sigma_{40}$ (cps)	$^{39}Ar \pm 2\sigma_{39}$ (cps)	$^{38}Ar \pm 2\sigma_{38}$ (cps)	$^{37}Ar \pm 2\sigma_{37}$ (cps)	$^{36}Ar \pm 2\sigma_{36}$ (cps)	$^{40}Ar^*/^{39}Ar_K \pm 2\sigma$	$\%^{40}Ar^*$	Age (Ma) ± 2σ (Ma)	K/Ca	Included in plateau
NAH8018	0.35	129947 ± 291	34079 ± 65	414 ± 7	150 ± 41	74.318 ± 5.026	3.149130 ± 0.033260	97.97	94.06 ± 0.97	92.22	YES
NAH8021	0.5	278108 ± 584	87675 ± 78	1050 ± 8	334 ± 40	6.420 ± 2.341	3.149921 ± 0.008003	99.30	94.09 ± 0.23	113.02	YES
NAH8023	0.65	263702 ± 551	83567 ± 111	1008 ± 11	328 ± 51	1.448 ± 2.544	3.150180 ± 0.009124	99.83	94.09 ± 0.27	109.55	YES
NAH8026	0.8	207515 ± 432	65299 ± 119	777 ± 13	310 ± 52	3.738 ± 3.756	3.152680 ± 0.016485	99.89	94.17 ± 0.48	108.74	YES
NAH8028	0.95	169458 ± 364	53692 ± 84	649 ± 9	212 ± 49	0.581 ± 2.961	3.152782 ± 0.036995	97.97	94.17 ± 1.08	112.13	YES
NAH8031	1.15	139088 ± 317	43617 ± 84	524 ± 9	188 ± 60	4.081 ± 3.173	3.153140 ± 0.021278	99.37	94.18 ± 0.62	106.51	YES
NAH8036	1.8	77512 ± 189	24085 ± 58	287 ± 7	92 ± 38	5.263 ± 2.983	3.160655 ± 0.017196	99.46	94.40 ± 0.50	90.72	YES
NAH8038	2.5	137316 ± 313	43275 ± 70	522 ± 9	175 ± 59	2.858 ± 3.081	3.160727 ± 0.021742	99.12	94.40 ± 0.63	99.63	YES
NAH8041	10	89292 ± 229	27778 ± 55	334 ± 7	130 ± 61	6.062 ± 3.093	3.161803 ± 0.044060	82.92	94.43 ± 1.28	97.94	YES

Plateau age (9 of 9): 94.15 ± 0.15 **MSWD: 0.29**
Inverse isochron age (9 of 9): 94.16 ± 0.28
$(^{40}Ar/^{36}Ar)_{trapped}$ intercept: 303 ± 32
Integrated age (9 of 9): 94.21 ± 0.18

Sample: **NC-B**
Material: **sanidine**

File	Laser Power (%)	$^{40}Ar \pm 2\sigma_{40}$ (cps)	$^{39}Ar \pm 2\sigma_{39}$ (cps)	$^{38}Ar \pm 2\sigma_{38}$ (cps)	$^{37}Ar \pm 2\sigma_{37}$ (cps)	$^{36}Ar \pm 2\sigma_{36}$ (cps)	$^{40}Ar^*/^{39}Ar_K \pm 2\sigma$	$\%^{40}Ar^*$	Age (Ma) ± 2σ (Ma)	K/Ca	Included in plateau
NAH8046	0.35	246109 ± 528	77026 ± 114	934 ± 11	308 ± 51	13.656 ± 2.764	3.142006 ± 0.010746	98.34	93.86 ± 0.31	107.51	YES
NAH8048	0.45	311111 ± 703	98999 ± 134	1205 ± 18	465 ± 51	0.372 ± 3.353	3.141295 ± 0.010148	99.96	93.83 ± 0.30	91.47	YES
NAH8051	0.55	335101 ± 695	106031 ± 116	1276 ± 13	462 ± 58	2.704 ± 3.058	3.152599 ± 0.008644	99.75	94.16 ± 0.25	98.70	YES
NAH8053	0.7	185224 ± 413	58822 ± 86	710 ± 10	265 ± 62	0.618 ± 3.248	3.145576 ± 0.016507	99.89	93.96 ± 0.48	95.49	YES
NAH8056	0.85	556325 ± 1153	175649 ± 142	2112 ± 16	752 ± 60	9.355 ± 3.175	3.151165 ± 0.005442	99.49	94.12 ± 0.16	100.40	YES
NAH8058	1.05	418808 ± 956	132287 ± 143	1602 ± 14	574 ± 58	6.184 ± 3.032	3.151766 ± 0.006889	99.55	94.14 ± 0.20	99.09	YES
NAH8061	1.3	102326 ± 251	31862 ± 64	380 ± 9	126 ± 57	6.984 ± 3.590	3.145902 ± 0.033657	97.95	93.97 ± 0.98	108.93	YES
NAH8063	1.8	2302 ± 51	454 ± 10	6 ± 3	3 ± 64	1.018 ± 3.259	4.399114 ± 2.142432	86.79	130.10 ± 61.16	65.62	YES

Plateau age (8 of 8): 94.07 ± 0.10 **MSWD: 1.08**
Inverse isochron age (8 of 8): 94.09 ± 0.45
$(^{40}Ar/^{36}Ar)_{trapped}$ intercept: 290 ± 130
Integrated age (8 of 8): 94.43 ± 0.11

Sample: **NC-B**
Material: **sanidine**

File	Laser Power (%)	$^{40}Ar \pm 2\sigma_{40}$ (cps)	$^{39}Ar \pm 2\sigma_{39}$ (cps)	$^{38}Ar \pm 2\sigma_{38}$ (cps)	$^{37}Ar \pm 2\sigma_{37}$ (cps)	$^{36}Ar \pm 2\sigma_{36}$ (cps)	$^{40}Ar^*/^{39}Ar_K \pm 2\sigma$	$\%^{40}Ar^*$	Age (Ma) ± 2σ (Ma)	K/Ca	Included in plateau
NAH8073	0.35	270273 ± 645	85161 ± 132	1037 ± 14	359 ± 53	11.015 ± 3.507	3.134853 ± 0.012327	98.78	93.65 ± 0.36	102.02	
NAH8076	0.45	344995 ± 810	109248 ± 144	1318 ± 14	449 ± 49	0.237 ± 2.633	3.157048 ± 0.007246	99.97	94.29 ± 0.21	104.70	YES
NAH8078	0.55	268215 ± 591	85087 ± 126	1034 ± 12	342 ± 67	1.218 ± 2.785	3.147773 ± 0.009809	99.86	94.02 ± 0.29	107.11	YES
NAH8081	0.7	294867 ± 636	92895 ± 124	1108 ± 13	368 ± 58	6.050 ± 3.175	3.154524 ± 0.010235	99.38	94.22 ± 0.30	108.51	YES
NAH8083	0.85	195258 ± 451	61255 ± 96	734 ± 11	277 ± 57	7.904 ± 3.695	3.148933 ± 0.018034	98.79	94.06 ± 0.53	94.92	YES
NAH8086	1.05	97172 ± 235	29966 ± 68	359 ± 6	129 ± 50	8.976 ± 3.006	3.153148 ± 0.029966	97.24	94.18 ± 0.87	100.14	YES
NAH8088	1.4	29232 ± 103	8771 ± 36	106 ± 5	26 ± 52	4.556 ± 3.328	3.177513 ± 0.113297	95.34	94.89 ± 3.30	146.14	YES
NAH8091	2.5	5230 ± 54	1214 ± 15	13 ± 3	1 ± 42	2.878 ± 3.185	3.598720 ± 0.783085	83.56	107.11 ± 22.64	435.19	YES

Plateau age (7 of 8): 94.19 ± 0.14 **MSWD: 0.68**
Inverse isochron age (7 of 8): 94.18 ± 0.50
$(^{40}Ar/^{36}Ar)_{trapped}$ intercept: 317 ± 140
Integrated age (8 of 8): 94.12 ± 0.16

Sample: **NC-B**
Material: **sanidine**

File	Laser Power (%)	$^{40}Ar \pm 2\sigma_{40}$ (cps) (cps)	$^{39}Ar \pm 2\sigma_{39}$ (cps) (cps)	$^{38}Ar \pm 2\sigma_{38}$ (cps) (cps)	$^{37}Ar \pm 2\sigma_{37}$ (cps) (cps)	$^{36}Ar \pm 2\sigma_{36}$ (cps) (cps)	$^{40}Ar^*/^{39}Ar_K$ ± 2σ	$\%^{40}Ar^*$	Age (Ma) ± 2σ (Ma)	K/Ca	Included in plateau
NAH8094	0.3	66043 ± 162	18454 ± 44	220 ± 6	92 ± 52	26.686 ± 3.349	3.146812 ± 0.054193	87.93	94.00 ± 1.58	86.04	YES
NAH8097	0.37	128485 ± 297	40333 ± 73	494 ± 7	171 ± 63	6.034 ± 3.055	3.140720 ± 0.022632	98.59	93.82 ± 0.66	101.24	YES
NAH8099	0.44	337813 ± 742	107153 ± 139	1299 ± 14	446 ± 41	3.385 ± 3.872	3.143009 ± 0.010820	99.69	93.88 ± 0.32	103.31	YES
NAH8101	0.51	484872 ± 1055	153720 ± 163	1849 ± 18	647 ± 51	0.235 ± 3.835	3.153596 ± 0.007487	99.98	94.19 ± 0.22	102.23	YES
NAH8103	0.6	108546 ± 272	34357 ± 70	417 ± 8	128 ± 38	2.075 ± 3.177	3.141057 ± 0.027624	99.42	93.83 ± 0.80	115.46	YES
NAH8105	0.75	103816 ± 260	32785 ± 70	391 ± 8	101 ± 72	3.247 ± 3.587	3.136686 ± 0.032678	99.06	93.70 ± 0.95	139.83	YES
NAH8107	0.95	76020 ± 198	24052 ± 61	283 ± 9	68 ± 53	1.119 ± 5.580	3.146430 ± 0.069271	99.55	93.98 ± 2.02	151.73	YES
NAH8109	1.35	70877 ± 196	22313 ± 57	268 ± 8	70 ± 62	3.864 ± 3.542	3.124540 ± 0.047406	98.36	93.35 ± 1.38	136.63	YES
NAH8112	10	89556 ± 243	27500 ± 67	321 ± 10	97 ± 53	8.136 ± 4.255	3.168029 ± 0.046208	97.28	94.61 ± 1.34	121.95	YES

Plateau age (9 of 9): **94.05 ± 0.17** **MSWD: 0.74**
Inverse isochron age (9 of 9): **94.06 ± 0.37**
$(^{40}Ar/^{36}Ar)_{trapped}$ intercept: **295 ± 58**
Integrated age (9 of 9): **93.99 ± 0.22**

Sample: **NC-B**
Material: **sanidine**

File	Laser Power (%)	$^{40}Ar \pm 2\sigma_{40}$ (cps) (cps)	$^{39}Ar \pm 2\sigma_{39}$ (cps) (cps)	$^{38}Ar \pm 2\sigma_{38}$ (cps) (cps)	$^{37}Ar \pm 2\sigma_{37}$ (cps) (cps)	$^{36}Ar \pm 2\sigma_{36}$ (cps) (cps)	$^{40}Ar^*/^{39}Ar_K$ ± 2σ	$\%^{40}Ar^*$	Age (Ma) ± 2σ (Ma)	K/Ca	Included in plateau
NAH8115	0.3	46924 ± 136	13453 ± 42	156 ± 6	63 ± 49	8.505 ± 3.309	3.299150 ± 0.073441	94.58	98.43 ± 2.13	91.11	
NAH8118	0.37	74339 ± 191	23337 ± 54	286 ± 7	102 ± 61	3.041 ± 3.207	3.146306 ± 0.041039	98.77	93.98 ± 1.19	98.06	YES
NAH8120	0.44	244551 ± 560	77543 ± 117	949 ± 14	377 ± 53	2.100 ± 4.492	3.145527 ± 0.017317	99.74	93.96 ± 0.50	88.49	YES
NAH8122	0.51	529123 ± 1157	168140 ± 185	2040 ± 19	807 ± 69	0.591 ± 4.469	3.145722 ± 0.007974	99.96	93.96 ± 0.23	89.60	YES
NAH8124	0.6	471933 ± 1038	149720 ± 185	1814 ± 16	699 ± 79	2.514 ± 3.683	3.146943 ± 0.007389	99.84	94.00 ± 0.22	92.07	YES
NAH8126	0.75	207119 ± 500	65280 ± 131	779 ± 14	302 ± 58	5.723 ± 4.189	3.146445 ± 0.019185	99.17	93.98 ± 0.56	93.08	YES
NAH8128	1	101142 ± 253	31697 ± 73	375 ± 8	141 ± 48	2.179 ± 3.463	3.170240 ± 0.032636	99.35	94.68 ± 0.95	96.74	YES
NAH8130	1.7	181851 ± 428	57357 ± 118	696 ± 13	271 ± 52	4.879 ± 4.425	3.144981 ± 0.023055	99.19	93.94 ± 0.67	90.86	YES
NAH8133	10	110109 ± 251	33263 ± 66	405 ± 7	147 ± 70	9.965 ± 3.044	3.220658 ± 0.027335	97.29	96.14 ± 0.79	97.19	

Plateau age (7 of 9): **93.99 ± 0.14** **MSWD: 0.36**
Inverse isochron age (7 of 9): **94.00 ± 1.90**
$(^{40}Ar/^{36}Ar)_{trapped}$ intercept: **347 ± 320**
Integrated age (9 of 9): **94.22 ± 0.16**

Sample: **NC-B**
Material: **sanidine**

File	Laser Power (%)	$^{40}Ar \pm 2\sigma_{40}$ (cps) (cps)	$^{39}Ar \pm 2\sigma_{39}$ (cps) (cps)	$^{38}Ar \pm 2\sigma_{38}$ (cps) (cps)	$^{37}Ar \pm 2\sigma_{37}$ (cps) (cps)	$^{36}Ar \pm 2\sigma_{36}$ (cps) (cps)	$^{40}Ar^*/^{39}Ar_K$ ± 2σ	$\%^{40}Ar^*$	Age (Ma) ± 2σ (Ma)	K/Ca	Included in plateau
NAH8136	0.3	60606 ± 159	16910 ± 52	199 ± 6	59 ± 49	16.613 ± 3.590	3.290522 ± 0.063402	91.81	98.17 ± 1.84	122.35	
NAH8139	0.38	302932 ± 624	93643 ± 121	1137 ± 12	342 ± 57	26.097 ± 3.499	3.151528 ± 0.011181	97.42	94.13 ± 0.33	117.91	YES
NAH8141	0.45	247946 ± 548	78372 ± 130	951 ± 15	279 ± 52	5.186 ± 4.248	3.143720 ± 0.016207	99.37	93.91 ± 0.47	120.76	YES
NAH8143	0.51	275917 ± 627	87455 ± 147	1066 ± 15	333 ± 57	3.558 ± 3.727	3.142597 ± 0.012754	99.61	93.87 ± 0.37	112.99	YES
NAH8145	0.6	127339 ± 294	40204 ± 83	481 ± 9	143 ± 68	2.287 ± 3.095	3.150060 ± 0.023003	99.46	94.09 ± 0.67	120.81	YES
NAH8147	0.75	136818 ± 318	43232 ± 74	522 ± 8	130 ± 54	2.551 ± 2.988	3.146813 ± 0.020659	99.43	94.00 ± 0.60	143.19	YES
NAH8149	1	70896 ± 182	22348 ± 49	272 ± 6	94 ± 58	1.296 ± 3.102	3.154850 ± 0.041449	99.45	94.23 ± 1.21	102.12	YES
NAH8151	2	229651 ± 525	72461 ± 109	865 ± 11	265 ± 64	5.763 ± 3.308	3.145325 ± 0.013657	99.24	93.95 ± 0.40	117.38	YES
NAH8154	12	83736 ± 221	23153 ± 51	288 ± 6	77 ± 64	31.752 ± 4.125	3.206930 ± 0.053208	88.67	95.74 ± 1.55	129.07	

Plateau age (7 of 9): **94.00 ± 0.18** **MSWD: 0.26**
Inverse isochron age (7 of 9): **93.91 ± 0.55**
$(^{40}Ar/^{36}Ar)_{trapped}$ intercept: **329 ± 110**
Integrated age (9 of 9): **94.23 ± 0.19**

Sample: **NC-B**
Material: **sanidine**

File	Laser Power (%)	$^{40}Ar \pm 2\sigma_{40}$ (cps) (cps)	$^{39}Ar \pm 2\sigma_{39}$ (cps) (cps)	$^{38}Ar \pm 2\sigma_{38}$ (cps) (cps)	$^{37}Ar \pm 2\sigma_{37}$ (cps) (cps)	$^{36}Ar \pm 2\sigma_{36}$ (cps) (cps)	$^{40}Ar^*/^{39}Ar_K$ ± 2σ	$\%^{40}Ar^*$	Age (Ma) ± 2σ (Ma)	K/Ca	Included in plateau
NAH8157	0.3	53944 ± 153	13563 ± 41	161 ± 6	169 ± 52	33.296 ± 4.010	3.244892 ± 0.088314	81.58	96.85 ± 2.57	34.50	
NAH8160	0.38	128141 ± 292	40166 ± 82	485 ± 9	507 ± 50	8.432 ± 3.405	3.128110 ± 0.025326	98.05	93.45 ± 0.74	34.07	
NAH8162	0.45	337209 ± 741	106574 ± 156	1276 ± 18	1111 ± 61	13.578 ± 4.641	3.126329 ± 0.013028	98.81	93.40 ± 0.38	41.24	
NAH8164	0.51	316294 ± 707	100601 ± 149	1211 ± 16	576 ± 51	2.463 ± 3.068	3.136649 ± 0.009146	99.76	93.70 ± 0.27	75.09	
NAH8166	0.6	328782 ± 752	104378 ± 227	1262 ± 17	436 ± 72	1.825 ± 3.181	3.144484 ± 0.009153	99.83	93.93 ± 0.27	102.96	
NAH8168	0.75	631658 ± 1367	200867 ± 229	2435 ± 19	712 ± 69	3.830 ± 4.833	3.138714 ± 0.007225	99.81	93.76 ± 0.21	121.33	
NAH8170	1.1	485192 ± 1039	153938 ± 201	1866 ± 19	533 ± 49	2.167 ± 4.429	3.147403 ± 0.008626	99.86	94.01 ± 0.25	124.29	
NAH8172	2.2	449624 ± 1036	141339 ± 174	1697 ± 18	453 ± 67	11.010 ± 3.976	3.157635 ± 0.008439	99.26	94.31 ± 0.25	134.07	
NAH8175	15	235636 ± 555	73710 ± 147	875 ± 12	260 ± 62	1.845 ± 3.194	3.189047 ± 0.012975	99.76	95.22 ± 0.38	122.11	

no plateau

Integrated age (9 of 9): **94.00 ± 0.11**

Sample: **NC-B**
Material: **sanidine**

File	Laser Power (%)	$^{40}Ar \pm 2\sigma_{40}$ (cps) (cps)	$^{39}Ar \pm 2\sigma_{39}$ (cps) (cps)	$^{38}Ar \pm 2\sigma_{38}$ (cps) (cps)	$^{37}Ar \pm 2\sigma_{37}$ (cps) (cps)	$^{36}Ar \pm 2\sigma_{36}$ (cps) (cps)	$^{40}Ar^*/^{39}Ar_K$ ± 2σ	$\%^{40}Ar^*$	Age (Ma) ± 2σ (Ma)	K/Ca	Included in plateau
NAH8178	0.3	40411 ± 117	11245 ± 39	135 ± 5	24 ± 55	13.378 ± 3.205	3.238061 ± 0.085102	90.11	96.65 ± 2.47	199.70	
NAH8181	0.38	120245 ± 286	37603 ± 117	463 ± 12	125 ± 63	6.039 ± 4.189	3.149511 ± 0.033286	98.49	94.07 ± 0.97	129.21	YES
NAH8183	0.45	234331 ± 540	74303 ± 125	905 ± 15	280 ± 46	1.249 ± 3.417	3.148483 ± 0.013761	99.83	94.04 ± 0.40	114.07	YES
NAH8185	0.51	291228 ± 626	92632 ± 113	1118 ± 11	331 ± 45	0.315 ± 2.459	3.142672 ± 0.007966	99.96	93.87 ± 0.23	120.16	YES
NAH8187	0.6	515275 ± 1148	163174 ± 201	1998 ± 19	588 ± 47	3.836 ± 3.913	3.150571 ± 0.007204	99.77	94.10 ± 0.21	119.33	YES
NAH8189	0.75	190664 ± 477	60651 ± 113	726 ± 13	210 ± 58	0.438 ± 4.089	3.141234 ± 0.020154	99.92	93.83 ± 0.59	124.21	YES
NAH8191	1.1	75690 ± 210	23099 ± 64	270 ± 8	67 ± 63	9.341 ± 3.907	3.155639 ± 0.050518	96.31	94.25 ± 1.47	148.72	YES
NAH8193	2.5	272666 ± 673	86092 ± 155	1038 ± 17	332 ± 64	6.227 ± 3.868	3.145325 ± 0.013449	99.31	93.95 ± 0.39	111.57	YES
NAH8196	15	23044 ± 90	6589 ± 28	80 ± 4	12 ± 66	6.339 ± 3.049	3.209636 ± 0.138161	91.78	95.82 ± 4.02	239.12	YES

Plateau age (8 of 9): **94.00 ± 0.14** **MSWD: 0.51**

Inverse isochron age (8 of 9): **93.97 ± 0.43**

$(^{40}Ar/^{36}Ar)_{trapped}$ intercept: **344 ± 150**

Integrated age (9 of 9): **94.08 ± 0.17**

Sample: **NC-B**
Material: **sanidine**

File	Laser Power (%)	$^{40}Ar \pm 2\sigma_{40}$ (cps) (cps)	$^{39}Ar \pm 2\sigma_{39}$ (cps) (cps)	$^{38}Ar \pm 2\sigma_{38}$ (cps) (cps)	$^{37}Ar \pm 2\sigma_{37}$ (cps) (cps)	$^{36}Ar \pm 2\sigma_{36}$ (cps) (cps)	$^{40}Ar^*/^{39}Ar_K$ ± 2σ	$\%^{40}Ar^*$	Age (Ma) ± 2σ (Ma)	K/Ca	Included in plateau
NAH8199	0.31	55519 ± 151	15416 ± 47	183 ± 5	51 ± 49	14.531 ± 3.491	3.319615 ± 0.067629	92.18	99.02 ± 1.96	130.13	
NAH8202	0.38	179077 ± 446	56571 ± 108	670 ± 11	152 ± 61	0.140 ± 3.291	3.164448 ± 0.017399	99.97	94.51 ± 0.51	159.78	YES
NAH8204	0.45	319335 ± 739	101009 ± 140	1214 ± 15	266 ± 51	2.712 ± 3.766	3.153093 ± 0.011163	99.74	94.18 ± 0.32	163.27	YES
NAH8206	0.5	200095 ± 468	63199 ± 120	781 ± 11	180 ± 46	3.557 ± 3.439	3.149024 ± 0.016275	99.46	94.06 ± 0.47	151.05	YES
NAH8208	0.57	140304 ± 337	44278 ± 90	532 ± 8	111 ± 54	0.923 ± 3.415	3.162164 ± 0.023051	99.79	94.44 ± 0.67	170.96	YES
NAH8210	0.75	40756 ± 123	12678 ± 47	148 ± 5	21 ± 35	2.855 ± 3.009	3.147172 ± 0.070880	97.90	94.01 ± 2.06	254.54	YES
NAH8212	1.2	33184 ± 103	9969 ± 36	121 ± 5	13 ± 33	4.863 ± 3.115	3.182797 ± 0.093311	95.61	95.04 ± 2.72	319.20	YES
NAH8214	15	7650 ± 52	2117 ± 16	26 ± 3	16 ± 48	4.969 ± 2.718	2.913180 ± 0.383409	80.61	87.18 ± 11.20	57.13	YES

Plateau age (7 of 8): **94.25 ± 0.22** **MSWD: 0.70**

Inverse isochron age (7 of 8): **94.31 ± 0.44**

$(^{40}Ar/^{36}Ar)_{trapped}$ intercept: **252 ± 180**

Integrated age (8 of 8): **94.47 ± 0.26**

Sample: **NC-B**
Material: **sanidine**

File	Laser Power (%)	$^{40}Ar \pm 2\sigma_{40}$ (cps)	$^{39}Ar \pm 2\sigma_{39}$ (cps)	$^{38}Ar \pm 2\sigma_{38}$ (cps)	$^{37}Ar \pm 2\sigma_{37}$ (cps)	$^{36}Ar \pm 2\sigma_{36}$ (cps)	$^{40}Ar^*/^{39}Ar_K$	± 2σ	$\%^{40}Ar^*$	Age (Ma)	± 2σ (Ma)	K/Ca	Included in plateau
NAH8219	0.32	157612 ± 340	46242 ± 83	562 ± 9	144 ± 58	35.212 ± 4.146	3.180811	± 0.026786	93.32	94.98	± 0.78	137.88	
NAH8222	0.39	298607 ± 588	94493 ± 112	1154 ± 12	334 ± 61	9.370 ± 3.494	3.130242	± 0.011065	99.06	93.51	± 0.32	121.78	
NAH8224	0.45	515228 ± 1162	163621 ± 166	1968 ± 19	615 ± 69	1.675 ± 3.723	3.145622	± 0.006839	99.90	93.96	± 0.20	114.38	YES
NAH8226	0.5	483573 ± 1096	153273 ± 215	1846 ± 19	614 ± 76	3.231 ± 4.262	3.148473	± 0.008346	99.79	94.04	± 0.24	107.32	YES
NAH8228	0.57	334435 ± 759	105776 ± 121	1262 ± 16	426 ± 65	2.735 ± 3.744	3.153789	± 0.010597	99.75	94.20	± 0.31	106.75	YES
NAH8230	0.75	156689 ± 365	49434 ± 83	592 ± 9	189 ± 48	3.782 ± 3.051	3.146620	± 0.018450	99.27	93.99	± 0.54	112.47	YES
NAH8232	1.2	164383 ± 400	51631 ± 98	622 ± 10	198 ± 62	4.034 ± 3.687	3.160231	± 0.021341	99.26	94.39	± 0.62	112.36	YES
NAH8234	15	25292 ± 92	7655 ± 27	88 ± 4	42 ± 45	2.270 ± 3.300	3.215170	± 0.128701	97.32	95.98	± 3.74	77.65	YES

Plateau age (6 of 8): **94.05 ± 0.14** **MSWD: 0.80**
Inverse isochron age (6 of 8): **94.00 ± 5.60**
$(^{40}Ar/^{36}Ar)_{trapped}$ intercept: **461 ± 450**
Integrated age (8 of 8): **94.08 ± 0.13**

Sample: **NC-B**
Material: **sanidine**

File	Laser Power (%)	$^{40}Ar \pm 2\sigma_{40}$ (cps)	$^{39}Ar \pm 2\sigma_{39}$ (cps)	$^{38}Ar \pm 2\sigma_{38}$ (cps)	$^{37}Ar \pm 2\sigma_{37}$ (cps)	$^{36}Ar \pm 2\sigma_{36}$ (cps)	$^{40}Ar^*/^{39}Ar_K$	± 2σ	$\%^{40}Ar^*$	Age (Ma)	± 2σ (Ma)	K/Ca	Included in plateau
NAH8815	0.4	404590 ± 822	123298 ± 145	1502 ± 16	443 ± 59	52.290 ± 4.572	3.154528	± 0.011095	96.13	94.22	± 0.32	119.58	YES
NAH8818	0.46	417826 ± 803	131721 ± 209	1590 ± 16	453 ± 69	7.814 ± 3.347	3.154074	± 0.007627	99.43	94.21	± 0.22	124.91	YES
NAH8820	0.52	234298 ± 508	74096 ± 148	888 ± 13	320 ± 63	2.614 ± 3.608	3.151341	± 0.014567	99.66	94.13	± 0.42	99.60	YES
NAH8822	0.6	168965 ± 380	53416 ± 110	627 ± 12	202 ± 43	2.083 ± 3.583	3.151322	± 0.020048	99.62	94.13	± 0.58	113.82	YES
NAH8824	0.8	146369 ± 348	46268 ± 123	545 ± 11	171 ± 56	4.096 ± 3.991	3.136846	± 0.025778	99.16	93.71	± 0.75	116.09	YES
NAH8826	1.5	148860 ± 342	46943 ± 116	562 ± 12	178 ± 51	3.132 ± 3.929	3.150914	± 0.025009	99.36	94.11	± 0.73	113.35	YES
NAH8828	5	156746 ± 366	49410 ± 131	581 ± 13	180 ± 46	4.136 ± 3.501	3.147072	± 0.021182	99.20	94.00	± 0.62	117.93	YES
NAH8829	9	25370 ± 82	7647 ± 32	95 ± 5	37 ± 60	2.998 ± 2.959	3.200520	± 0.115541	96.47	95.56	± 3.36	89.42	YES

Plateau age (8 of 8): **94.16 ± 0.15** **MSWD: 0.40**
Inverse isochron age (8 of 8): **94.14 ± 0.41**
$(^{40}Ar/^{36}Ar)_{trapped}$ intercept: **308 ± 61**
Integrated age (8 of 8): **94.14 ± 0.17**

Sample: **NC-C**
Material: **sanidine**

File	Laser Power (%)	$^{40}Ar \pm 2\sigma_{40}$ (cps)	$^{39}Ar \pm 2\sigma_{39}$ (cps)	$^{38}Ar \pm 2\sigma_{38}$ (cps)	$^{37}Ar \pm 2\sigma_{37}$ (cps)	$^{36}Ar \pm 2\sigma_{36}$ (cps)	$^{40}Ar^*/^{39}Ar_K$	± 2σ	$\%^{40}Ar^*$	Age (Ma)	± 2σ (Ma)	K/Ca	Included in plateau
NAH8266	0.32	108725 ± 249	32716 ± 82	389 ± 7	127 ± 61	12.336 ± 3.366	3.210519	± 0.030736	96.61	95.85	± 0.89	110.72	
NAH8269	0.39	317197 ± 663	100090 ± 163	1211 ± 17	363 ± 48	6.259 ± 3.535	3.150207	± 0.010579	99.40	94.09	± 0.31	118.53	
NAH8271	0.45	543977 ± 1172	172095 ± 184	2086 ± 21	687 ± 68	1.775 ± 3.449	3.157623	± 0.006032	99.90	94.31	± 0.18	107.76	
NAH8273	0.5	538841 ± 1178	169856 ± 238	2064 ± 18	634 ± 55	2.099 ± 3.444	3.168416	± 0.006109	99.88	94.62	± 0.18	115.28	
NAH8275	0.7	176847 ± 400	55390 ± 78	665 ± 9	215 ± 49	3.720 ± 3.071	3.172457	± 0.016573	99.36	94.74	± 0.48	110.62	
NAH8277	1	101814 ± 248	31686 ± 61	380 ± 7	131 ± 58	3.562 ± 3.216	3.179429	± 0.030317	98.95	94.94	± 0.88	103.88	
NAH8279	15	25772 ± 92	7897 ± 35	91 ± 4	29 ± 45	4.293 ± 3.342	3.100939	± 0.126351	95.02	92.66	± 3.68	118.82	

no plateau

Integrated age (7 of 7): **94.51 ± 0.14**

Sample: **NC-C**
Material: **sanidine**

File	Laser Power (%)	$^{40}Ar \pm 2\sigma_{40}$ (cps) (cps)	$^{39}Ar \pm 2\sigma_{39}$ (cps) (cps)	$^{38}Ar \pm 2\sigma_{38}$ (cps) (cps)	$^{37}Ar \pm 2\sigma_{37}$ (cps) (cps)	$^{36}Ar \pm 2\sigma_{36}$ (cps) (cps)	$^{40}Ar^*/^{39}Ar_K$ ± 2σ	$\%^{40}Ar^*$	Age (Ma) ± 2σ (Ma)	K/Ca	Included in plateau
NAH8287	0.32	239925 ± 580	73875 ± 102	880 ± 11	296 ± 56	14.097 ± 3.369	3.190510 ± 0.013644	98.24	95.27 ± 0.40	107.25	
NAH8290	0.39	315417 ± 709	99562 ± 121	1223 ± 10	396 ± 46	5.514 ± 2.380	3.151286 ± 0.007183	99.47	94.13 ± 0.21	108.02	YES
NAH8292	0.44	257069 ± 594	81415 ± 124	990 ± 14	358 ± 58	3.430 ± 2.465	3.144760 ± 0.009083	99.60	93.94 ± 0.26	97.83	YES
NAH8294	0.48	534240 ± 1181	169021 ± 204	2049 ± 16	757 ± 62	7.319 ± 3.519	3.147688 ± 0.006268	99.59	94.02 ± 0.18	96.00	YES
NAH8296	0.52	288267 ± 640	91065 ± 183	1098 ± 12	371 ± 49	5.947 ± 3.123	3.145809 ± 0.010282	99.38	93.97 ± 0.30	105.56	YES
NAH8298	0.59	165035 ± 381	51953 ± 99	627 ± 10	215 ± 56	2.957 ± 3.018	3.159391 ± 0.017367	99.46	94.36 ± 0.51	103.97	YES
NAH8300	0.75	90218 ± 235	28303 ± 74	343 ± 8	125 ± 53	3.520 ± 2.975	3.150261 ± 0.031406	98.83	94.10 ± 0.91	97.73	YES
NAH8302	1.5	96146 ± 225	30132 ± 62	358 ± 6	108 ± 43	3.983 ± 2.916	3.151071 ± 0.028908	98.75	94.12 ± 0.84	119.94	YES
NAH8305	13	172457 ± 375	53445 ± 88	642 ± 10	231 ± 45	5.322 ± 3.148	3.196912 ± 0.017608	99.07	95.45 ± 0.51	99.32	

Plateau age (7 of 9): 94.05 ± 0.11 **MSWD: 0.54**
Inverse isochron age (7 of 9): 93.90 ± 1.40
$(^{40}Ar/^{36}Ar)_{trapped}$ intercept: 393 ± 480
Integrated age (9 of 9): 94.30 ± 0.12

Sample: **NC-C**
Material: **sanidine**

File	Laser Power (%)	$^{40}Ar \pm 2\sigma_{40}$ (cps) (cps)	$^{39}Ar \pm 2\sigma_{39}$ (cps) (cps)	$^{38}Ar \pm 2\sigma_{38}$ (cps) (cps)	$^{37}Ar \pm 2\sigma_{37}$ (cps) (cps)	$^{36}Ar \pm 2\sigma_{36}$ (cps) (cps)	$^{40}Ar^*/^{39}Ar_K$ ± 2σ	$\%^{40}Ar^*$	Age (Ma) ± 2σ (Ma)	K/Ca	Included in plateau
NAH8315	0.48	13641 ± 71	4106 ± 28	48 ± 4	55 ± 53	3.320 ± 3.081	3.081157 ± 0.224073	92.75	92.08 ± 6.53	32.23	
NAH8317	0.52	17519 ± 72	5323 ± 30	65 ± 5	36 ± 53	3.610 ± 3.226	3.088926 ± 0.180964	93.85	92.31 ± 5.27	63.39	
NAH8319	0.59	40001 ± 118	12660 ± 43	155 ± 5	64 ± 54	2.668 ± 2.900	3.096567 ± 0.068416	98.00	92.53 ± 1.99	85.20	
NAH8321	0.75	248376 ± 551	79572 ± 122	977 ± 15	266 ± 65	5.250 ± 3.528	3.101459 ± 0.013266	99.36	92.67 ± 0.39	128.56	
NAH8323	1.5	476407 ± 988	151560 ± 161	1856 ± 13	575 ± 71	0.122 ± 2.184	3.142894 ± 0.004366	99.98	93.88 ± 0.13	113.37	
NAH8326	13	584354 ± 1196	183973 ± 150	2246 ± 15	749 ± 65	8.160 ± 3.232	3.162860 ± 0.005291	99.58	94.46 ± 0.15	105.57	
NAH8350	18	169800 ± 383	52527 ± 83	626 ± 8	212 ± 59	8.395 ± 3.029	3.184688 ± 0.017239	98.52	95.10 ± 0.50	106.50	
NAH8353	23	26806 ± 95	7662 ± 34	89 ± 4	35 ± 57	6.483 ± 2.818	3.245838 ± 0.109816	92.77	96.88 ± 3.19	94.28	

no plateau
Integrated age (8 of 8): 94.01 ± 0.15

Sample: **NC-C**
Material: **sanidine**

File	Laser Power (%)	$^{40}Ar \pm 2\sigma_{40}$ (cps) (cps)	$^{39}Ar \pm 2\sigma_{39}$ (cps) (cps)	$^{38}Ar \pm 2\sigma_{38}$ (cps) (cps)	$^{37}Ar \pm 2\sigma_{37}$ (cps) (cps)	$^{36}Ar \pm 2\sigma_{36}$ (cps) (cps)	$^{40}Ar^*/^{39}Ar_K$ ± 2σ	$\%^{40}Ar^*$	Age (Ma) ± 2σ (Ma)	K/Ca	Included in plateau
NAH8329	0.32	25166 ± 90	6910 ± 31	80 ± 4	42 ± 53	9.481 ± 3.273	3.232112 ± 0.141429	88.75	96.48 ± 4.11	71.09	
NAH8332	0.39	44030 ± 139	13705 ± 45	172 ± 7	77 ± 65	5.339 ± 3.242	3.096283 ± 0.070633	96.38	92.52 ± 2.06	76.36	
NAH8334	0.44	22784 ± 93	7130 ± 30	83 ± 5	25 ± 43	3.163 ± 3.422	3.062913 ± 0.143303	95.85	91.55 ± 4.18	121.91	
NAH8336	0.48	162443 ± 425	51930 ± 101	636 ± 11	205 ± 60	5.949 ± 3.433	3.093677 ± 0.019765	98.90	92.45 ± 0.58	108.71	
NAH8338	0.52	105813 ± 249	33812 ± 80	407 ± 8	160 ± 40	3.744 ± 3.072	3.096246 ± 0.027143	98.94	92.52 ± 0.79	90.64	
NAH8340	0.59	75105 ± 187	23949 ± 57	292 ± 7	107 ± 53	5.592 ± 2.881	3.066117 ± 0.035930	97.77	91.64 ± 1.05	95.89	
NAH8342	0.75	329357 ± 723	104999 ± 139	1277 ± 14	443 ± 55	4.125 ± 3.289	3.124828 ± 0.009387	99.62	93.36 ± 0.27	101.99	
NAH8344	1.5	138220 ± 327	43914 ± 89	535 ± 8	199 ± 47	1.593 ± 3.052	3.136478 ± 0.020774	99.65	93.69 ± 0.60	95.10	
NAH8347	13	166547 ± 377	51836 ± 99	627 ± 10	246 ± 47	10.475 ± 3.097	3.152499 ± 0.017862	98.12	94.16 ± 0.52	90.78	
NAH8356	20	17496 ± 72	4295 ± 25	54 ± 5	25 ± 69	13.488 ± 2.874	3.135865 ± 0.199836	76.98	93.68 ± 5.82	75.09	

no plateau
Integrated age (10 of 10): 93.18 ± 0.25

Sample: **NC-C**
Material: **sanidine**

File	Laser Power (%)	$^{40}Ar \pm 2\sigma_{40}$ (cps) (cps)	$^{39}Ar \pm 2\sigma_{39}$ (cps) (cps)	$^{38}Ar \pm 2\sigma_{38}$ (cps) (cps)	$^{37}Ar \pm 2\sigma_{37}$ (cps) (cps)	$^{36}Ar \pm 2\sigma_{36}$ (cps) (cps)	$^{40}Ar^*/^{39}Ar_K$ ± 2σ	$\%^{40}Ar^*$	Age (Ma) ± 2σ (Ma)	K/Ca	Included in plateau
NAH8359	0.33	138120 ± 355	42801 ± 97	511 ± 11	196 ± 57	11.510 ± 4.044	3.146554 ± 0.028231	97.51	93.99 ± 0.82	93.98	YES
NAH8362	0.4	386281 ± 825	121464 ± 147	1482 ± 15	508 ± 55	15.024 ± 3.664	3.143084 ± 0.009039	98.83	93.89 ± 0.26	102.85	YES
NAH8364	0.44	250520 ± 561	79101 ± 133	956 ± 13	334 ± 57	5.436 ± 3.364	3.146364 ± 0.012729	99.35	93.98 ± 0.37	101.69	YES
NAH8366	0.48	104755 ± 256	32830 ± 65	389 ± 10	135 ± 54	4.770 ± 3.561	3.147254 ± 0.032398	98.63	94.01 ± 0.94	104.89	YES
NAH8368	0.55	28887 ± 105	8885 ± 35	104 ± 6	46 ± 60	1.824 ± 2.974	3.189848 ± 0.099937	98.11	95.25 ± 2.91	83.70	YES
NAH8370	20	12304 ± 66	3691 ± 23	42 ± 5	19 ± 44	2.843 ± 2.925	3.103496 ± 0.236621	93.10	92.73 ± 6.89	83.40	YES

Plateau age (6 of 6): **93.93 ± 0.21** **MSWD: 0.24**
Inverse isochron age (6 of 6): **93.90 ± 2.30**
$(^{40}Ar/^{36}Ar)_{trapped}$ intercept: **300 ± 240**
Integrated age (6 of 6): **93.97 ± 0.25**

Sample: **NC-C**
Material: **sanidine**

File	Laser Power (%)	$^{40}Ar \pm 2\sigma_{40}$ (cps) (cps)	$^{39}Ar \pm 2\sigma_{39}$ (cps) (cps)	$^{38}Ar \pm 2\sigma_{38}$ (cps) (cps)	$^{37}Ar \pm 2\sigma_{37}$ (cps) (cps)	$^{36}Ar \pm 2\sigma_{36}$ (cps) (cps)	$^{40}Ar^*/^{39}Ar_K$ ± 2σ	$\%^{40}Ar^*$	Age (Ma) ± 2σ (Ma)	K/Ca	Included in plateau
NAH8383	0.4	201797 ± 474	63523 ± 143	773 ± 15	269 ± 61	4.614 ± 3.988	3.154864 ± 0.018770	99.31	94.23 ± 0.55	101.37	YES
NAH8385	0.44	86736 ± 238	27378 ± 83	325 ± 9	93 ± 69	2.830 ± 3.652	3.136940 ± 0.039845	99.02	93.71 ± 1.16	125.98	YES
NAH8387	0.48	97034 ± 265	30607 ± 76	369 ± 9	125 ± 59	4.252 ± 4.203	3.128670 ± 0.041015	98.68	93.47 ± 1.19	105.20	YES
NAH8389	0.52	118042 ± 306	37143 ± 95	444 ± 9	147 ± 53	3.620 ± 3.648	3.148700 ± 0.029342	99.08	94.05 ± 0.85	108.77	YES
NAH8391	0.6	74268 ± 198	23263 ± 53	275 ± 7	110 ± 66	4.984 ± 3.090	3.128348 ± 0.039675	97.99	93.46 ± 1.16	91.09	YES
NAH8393	0.8	51019 ± 147	15994 ± 43	191 ± 6	66 ± 34	2.090 ± 3.159	3.150696 ± 0.058989	98.77	94.11 ± 1.72	104.89	YES
NAH8395	1.5	68621 ± 203	20302 ± 56	245 ± 7	64 ± 41	15.501 ± 4.097	3.151755 ± 0.060261	93.25	94.14 ± 1.75	136.04	YES
NAH8398	15	90224 ± 243	27722 ± 58	330 ± 7	87 ± 40	7.589 ± 3.356	3.172530 ± 0.036163	97.48	94.74 ± 1.05	137.45	YES

Plateau age (8 of 8): **94.07 ± 0.35** **MSWD: 0.65**
Inverse isochron age (8 of 8): **94.00 ± 1.10**
$(^{40}Ar/^{36}Ar)_{trapped}$ intercept: **315 ± 140**
Integrated age (8 of 8): **94.02 ± 0.37**

Sample: **NC-C**
Material: **sanidine**

File	Laser Power (%)	$^{40}Ar \pm 2\sigma_{40}$ (cps) (cps)	$^{39}Ar \pm 2\sigma_{39}$ (cps) (cps)	$^{38}Ar \pm 2\sigma_{38}$ (cps) (cps)	$^{37}Ar \pm 2\sigma_{37}$ (cps) (cps)	$^{36}Ar \pm 2\sigma_{36}$ (cps) (cps)	$^{40}Ar^*/^{39}Ar_K$ ± 2σ	$\%^{40}Ar^*$	Age (Ma) ± 2σ (Ma)	K/Ca	Included in plateau
NAH8404	0.33	51636 ± 141	13928 ± 45	167 ± 6	98 ± 46	17.672 ± 3.454	3.328495 ± 0.074049	89.78	99.28 ± 2.15	61.26	
NAH8407	0.4	74636 ± 181	23408 ± 58	285 ± 6	94 ± 53	3.747 ± 2.920	3.140400 ± 0.037266	98.49	93.81 ± 1.09	106.93	YES
NAH8409	0.44	36011 ± 108	11094 ± 43	136 ± 5	37 ± 59	2.446 ± 3.094	3.179792 ± 0.083289	97.96	94.96 ± 2.42	130.66	YES
NAH8411	0.48	245447 ± 531	78097 ± 110	956 ± 12	341 ± 51	0.561 ± 2.972	3.140524 ± 0.011393	99.93	93.81 ± 0.33	98.62	YES
NAH8413	0.52	176736 ± 408	56033 ± 96	691 ± 12	205 ± 70	1.570 ± 2.960	3.145550 ± 0.015796	99.73	93.96 ± 0.46	117.59	YES
NAH8415	0.6	170703 ± 395	53915 ± 93	644 ± 12	232 ± 72	1.770 ± 3.519	3.156143 ± 0.019510	99.68	94.27 ± 0.57	100.02	YES
NAH8417	0.85	131637 ± 309	41469 ± 94	504 ± 10	153 ± 69	2.638 ± 3.732	3.155120 ± 0.026892	99.39	94.24 ± 0.78	116.46	YES
NAH8419	2	127328 ± 320	39815 ± 84	484 ± 9	144 ± 56	6.839 ± 3.269	3.146429 ± 0.024533	98.39	93.98 ± 0.71	118.76	YES
NAH8422	15	3166 ± 48	214 ± 8	4 ± 4	12 ± 51	8.170 ± 3.069	3.396951 ± 4.299474	22.99	101.26 ± 124.69	7.91	YES

Plateau age (8 of 9): **93.97 ± 0.22** **MSWD: 0.46**
Inverse isochron age (8 of 9): **93.97 ± 0.40**
$(^{40}Ar/^{36}Ar)_{trapped}$ intercept: **326 ± 160**
Integrated age (9 of 9): **94.28 ± 0.26**

Sample: **NC-C**
Material: **sanidine**

File	Laser Power (%)	$^{40}Ar \pm 2\sigma_{40}$ (cps)	$^{39}Ar \pm 2\sigma_{39}$ (cps)	$^{38}Ar \pm 2\sigma_{38}$ (cps)	$^{37}Ar \pm 2\sigma_{37}$ (cps)	$^{36}Ar \pm 2\sigma_{36}$ (cps)	$^{40}Ar^*/^{39}Ar_K$ ± 2σ	$\%^{40}Ar^*$	Age (Ma) ± 2σ (Ma)	K/Ca	Included in plateau
NAH8425	0.33	31412 ± 105	8631 ± 33	98 ± 5	29 ± 58	7.440 ± 3.247	3.381757 ± 0.112347	92.92	100.82 ± 3.26	126.73	
NAH8428	0.4	58170 ± 167	18088 ± 49	216 ± 6	58 ± 76	2.702 ± 2.972	3.171106 ± 0.049075	98.60	94.70 ± 1.43	134.92	
NAH8430	0.44	41866 ± 126	13028 ± 43	157 ± 6	31 ± 42	2.599 ± 3.040	3.153697 ± 0.069692	98.14	94.20 ± 2.03	182.31	
NAH8432	0.48	179589 ± 422	56758 ± 119	678 ± 11	218 ± 60	1.068 ± 3.934	3.158278 ± 0.020717	99.81	94.33 ± 0.60	112.04	
NAH8434	0.52	164215 ± 377	52480 ± 109	639 ± 12	213 ± 45	4.083 ± 3.842	3.105688 ± 0.021882	99.25	92.80 ± 0.64	105.94	
NAH8436	0.6	128183 ± 309	40964 ± 82	491 ± 10	173 ± 51	1.581 ± 3.437	3.117431 ± 0.025070	99.62	93.14 ± 0.73	102.02	
NAH8438	0.85	632348 ± 1381	200305 ± 211	2424 ± 24	816 ± 63	3.777 ± 4.009	3.151091 ± 0.006025	99.81	94.12 ± 0.18	105.49	
NAH8440	2	209015 ± 446	65913 ± 103	798 ± 11	226 ± 59	4.647 ± 2.973	3.149765 ± 0.013493	99.33	94.08 ± 0.39	125.24	
NAH8443	15	161011 ± 341	49504 ± 78	594 ± 9	163 ± 62	8.938 ± 3.497	3.198281 ± 0.021105	98.33	95.49 ± 0.61	130.68	
NAH8510	22	11520 ± 69	3095 ± 21	34 ± 4	10 ± 50	6.327 ± 2.918	3.111171 ± 0.281484	83.59	92.96 ± 8.20	131.20	

no plateau

Integrated age (10 of 10): **94.19 ± 0.18**

Sample: **NC-C**
Material: **sanidine**

File	Laser Power (%)	$^{40}Ar \pm 2\sigma_{40}$ (cps)	$^{39}Ar \pm 2\sigma_{39}$ (cps)	$^{38}Ar \pm 2\sigma_{38}$ (cps)	$^{37}Ar \pm 2\sigma_{37}$ (cps)	$^{36}Ar \pm 2\sigma_{36}$ (cps)	$^{40}Ar^*/^{39}Ar_K$ ± 2σ	$\%^{40}Ar^*$	Age (Ma) ± 2σ (Ma)	K/Ca	Included in plateau
NAH8446	0.33	28010 ± 106	7188 ± 41	82 ± 5	42 ± 67	11.534 ± 3.421	3.417373 ± 0.142106	87.70	101.86 ± 4.12	73.52	
NAH8449	0.4	45830 ± 126	14223 ± 44	170 ± 6	35 ± 48	4.820 ± 3.135	3.120791 ± 0.065826	96.85	93.24 ± 1.92	177.00	YES
NAH8451	0.44	62047 ± 180	19703 ± 62	239 ± 8	83 ± 50	0.941 ± 3.437	3.134664 ± 0.052093	99.54	93.64 ± 1.52	102.15	YES
NAH8453	0.48	111678 ± 274	35403 ± 84	425 ± 9	166 ± 46	0.696 ± 3.438	3.148486 ± 0.029010	99.81	94.04 ± 0.84	91.60	YES
NAH8455	0.52	163508 ± 381	51863 ± 97	616 ± 12	194 ± 73	1.661 ± 3.516	3.142884 ± 0.020266	99.69	93.88 ± 0.59	114.71	YES
NAH8457	0.6	234701 ± 519	74520 ± 114	883 ± 15	274 ± 93	1.206 ± 3.688	3.144418 ± 0.014799	99.84	93.93 ± 0.43	117.12	YES
NAH8459	0.85	462861 ± 990	147064 ± 159	1797 ± 17	643 ± 63	1.047 ± 3.531	3.145040 ± 0.007209	99.93	93.94 ± 0.21	98.29	YES
NAH8461	2	221959 ± 499	70119 ± 110	834 ± 11	310 ± 47	2.053 ± 3.299	3.156512 ± 0.014075	99.72	94.28 ± 0.41	97.13	YES
NAH8464	15	327467 ± 708	102584 ± 130	1229 ± 16	436 ± 62	7.738 ± 3.523	3.169457 ± 0.010284	99.29	94.65 ± 0.30	101.13	
NAH8513	22	3122 ± 53	501 ± 11	7 ± 4	7 ± 70	4.579 ± 3.058	3.501092 ± 1.822392	56.21	104.28 ± 52.76	32.54	

Plateau age (7 of 10): **93.98 ± 0.16** **MSWD: 0.54**

Inverse isochron age (7 of 10): **94.02 ± 0.75**

$(^{40}Ar/^{36}Ar)_{trapped}$ intercept: **270 ± 320**

Integrated age (10 of 10): **94.21 ± 0.18**

Sample: **NC-C**
Material: **sanidine**

File	Laser Power (%)	$^{40}Ar \pm 2\sigma_{40}$ (cps)	$^{39}Ar \pm 2\sigma_{39}$ (cps)	$^{38}Ar \pm 2\sigma_{38}$ (cps)	$^{37}Ar \pm 2\sigma_{37}$ (cps)	$^{36}Ar \pm 2\sigma_{36}$ (cps)	$^{40}Ar^*/^{39}Ar_K$ ± 2σ	$\%^{40}Ar^*$	Age (Ma) ± 2σ (Ma)	K/Ca	Included in plateau
NAH8467	0.32	25723 ± 89	6838 ± 31	80 ± 5	9 ± 60	8.691 ± 3.075	3.381619 ± 0.134292	89.90	100.82 ± 3.90	310.64	
NAH8470	0.4	45622 ± 129	14149 ± 47	170 ± 6	29 ± 51	2.369 ± 3.101	3.173906 ± 0.065444	98.44	94.78 ± 1.90	211.93	
NAH8472	0.44	47678 ± 130	15014 ± 45	185 ± 6	62 ± 57	4.129 ± 3.065	3.093351 ± 0.060961	97.41	92.44 ± 1.78	104.30	
NAH8474	0.48	55650 ± 152	17704 ± 48	215 ± 7	70 ± 65	3.660 ± 2.991	3.081352 ± 0.050463	98.03	92.09 ± 1.47	108.36	
NAH8476	0.52	34349 ± 106	10783 ± 43	130 ± 6	45 ± 49	1.271 ± 2.717	3.150176 ± 0.075234	98.89	94.09 ± 2.19	103.55	YES
NAH8478	0.6	270091 ± 616	85890 ± 120	1034 ± 15	367 ± 78	1.588 ± 3.712	3.138912 ± 0.012933	99.82	93.77 ± 0.38	100.56	YES
NAH8480	0.85	424385 ± 934	134875 ± 198	1625 ± 20	625 ± 78	2.361 ± 3.898	3.141119 ± 0.008669	99.83	93.83 ± 0.25	92.78	YES
NAH8482	2	590086 ± 1364	186809 ± 203	2232 ± 23	841 ± 52	5.220 ± 3.815	3.150252 ± 0.006150	99.73	94.10 ± 0.18	95.47	YES
NAH8485	15	200614 ± 458	52804 ± 91	644 ± 9	264 ± 41	116.222 ± 5.872	3.141947 ± 0.033227	82.70	93.85 ± 0.97	85.91	YES

Plateau age (8 of 9): **93.97 ± 0.14** **MSWD: 1.11**

Inverse isochron age (8 of 9): **93.98 ± 0.29**

$(^{40}Ar/^{36}Ar)_{trapped}$ intercept: **297 ± 24**

Integrated age (9 of 9): **93.94 ± 0.18**

Sample: **NC-C**
Material: **sanidine**

File	Laser Power (%)	$^{40}Ar \pm 2\sigma_{40}$ (cps) (cps)	$^{39}Ar \pm 2\sigma_{39}$ (cps) (cps)	$^{38}Ar \pm 2\sigma_{38}$ (cps) (cps)	$^{37}Ar \pm 2\sigma_{37}$ (cps) (cps)	$^{36}Ar \pm 2\sigma_{36}$ (cps) (cps)	$^{40}Ar^*/^{39}Ar_K$ ± 2σ	$\%^{40}Ar^*$	Age (Ma) ± 2σ (Ma)	K/Ca	Included in plateau
NAH8488	0.33	27134 ± 98	7596 ± 36	88 ± 5	41 ± 49	5.480 ± 3.082	3.356617 ± 0.121150	93.97	100.09 ± 3.52	78.71	
NAH8491	0.4	25669 ± 94	7852 ± 32	97 ± 4	30 ± 54	0.752 ± 3.011	3.240254 ± 0.114505	99.12	96.71 ± 3.33	113.12	YES
NAH8493	0.44	48227 ± 142	14967 ± 42	179 ± 6	61 ± 56	2.929 ± 3.135	3.163613 ± 0.062546	98.18	94.48 ± 1.82	104.76	YES
NAH8495	0.48	31748 ± 93	9948 ± 36	118 ± 5	28 ± 50	1.504 ± 2.740	3.145855 ± 0.082248	98.58	93.97 ± 2.39	152.49	YES
NAH8497	0.52	51596 ± 138	16287 ± 46	198 ± 6	46 ± 48	2.649 ± 3.201	3.119115 ± 0.058689	98.46	93.19 ± 1.71	153.11	YES
NAH8499	0.6	212941 ± 509	67515 ± 168	812 ± 15	287 ± 70	1.403 ± 3.956	3.147574 ± 0.017529	99.80	94.02 ± 0.51	101.02	YES
NAH8501	0.85	347046 ± 782	110022 ± 199	1345 ± 16	416 ± 64	1.014 ± 3.599	3.151368 ± 0.009809	99.91	94.13 ± 0.29	113.79	YES
NAH8503	2	291512 ± 648	91836 ± 200	1105 ± 15	340 ± 63	8.039 ± 4.462	3.147884 ± 0.014539	99.17	94.03 ± 0.42	115.98	YES
NAH8506	15	47356 ± 132	14173 ± 46	166 ± 6	64 ± 45	8.570 ± 3.422	3.160567 ± 0.072096	94.59	94.40 ± 2.10	95.36	YES

Plateau age (8 of 9): **94.09 ± 0.21** **MSWD: 0.59**
Inverse isochron age (8 of 9): **94.08 ± 0.65**
$(^{40}Ar/^{36}Ar)_{trapped}$ intercept: **315 ± 180**
Integrated age (9 of 9): **94.25 ± 0.26**

Sample: **NC-C**
Material: **sanidine**

File	Laser Power (%)	$^{40}Ar \pm 2\sigma_{40}$ (cps) (cps)	$^{39}Ar \pm 2\sigma_{39}$ (cps) (cps)	$^{38}Ar \pm 2\sigma_{38}$ (cps) (cps)	$^{37}Ar \pm 2\sigma_{37}$ (cps) (cps)	$^{36}Ar \pm 2\sigma_{36}$ (cps) (cps)	$^{40}Ar^*/^{39}Ar_K$ ± 2σ	$\%^{40}Ar^*$	Age (Ma) ± 2σ (Ma)	K/Ca	Included in plateau
NAH8796	0.4	214977 ± 483	66832 ± 128	805 ± 10	318 ± 46	13.503 ± 3.595	3.156215 ± 0.016087	98.12	94.27 ± 0.47	90.42	YES
NAH8799	0.46	287161 ± 610	90792 ± 133	1091 ± 14	348 ± 68	5.828 ± 3.762	3.143429 ± 0.012398	99.39	93.90 ± 0.36	112.33	YES
NAH8801	0.52	184455 ± 422	58401 ± 111	706 ± 13	249 ± 61	2.395 ± 3.629	3.145981 ± 0.018577	99.61	93.97 ± 0.54	100.66	YES
NAH8803	0.6	70238 ± 204	22167 ± 51	264 ± 8	92 ± 56	0.885 ± 3.534	3.156455 ± 0.047615	99.62	94.28 ± 1.39	103.27	YES
NAH8805	0.8	114064 ± 277	35355 ± 70	437 ± 9	153 ± 53	10.507 ± 3.339	3.137358 ± 0.028217	97.24	93.72 ± 0.82	99.22	YES
NAH8807	1.5	63483 ± 181	19834 ± 61	239 ± 7	71 ± 56	3.893 ± 3.185	3.141799 ± 0.047960	98.16	93.85 ± 1.40	120.63	YES
NAH8809	5	137651 ± 343	43491 ± 90	517 ± 11	174 ± 68	1.184 ± 3.319	3.156659 ± 0.022808	99.74	94.28 ± 0.66	107.67	YES

Plateau age (7 of 7): **94.03 ± 0.22** **MSWD: 0.50**
Inverse isochron age (7 of 7): **94.03 ± 0.82**
$(^{40}Ar/^{36}Ar)_{trapped}$ intercept: **305 ± 160**
Integrated age (7 of 7): **94.04 ± 0.24**

Sample: **NC-D**
Material: **sanidine**

File	Laser Power (%)	$^{40}Ar \pm 2\sigma_{40}$ (cps) (cps)	$^{39}Ar \pm 2\sigma_{39}$ (cps) (cps)	$^{38}Ar \pm 2\sigma_{38}$ (cps) (cps)	$^{37}Ar \pm 2\sigma_{37}$ (cps) (cps)	$^{36}Ar \pm 2\sigma_{36}$ (cps) (cps)	$^{40}Ar^*/^{39}Ar_K$ ± 2σ	$\%^{40}Ar^*$	Age (Ma) ± 2σ (Ma)	K/Ca	Included in plateau
NAH8521	0.33	15806 ± 82	3828 ± 26	43 ± 4	33 ± 63	11.142 ± 3.425	3.259942 ± 0.267191	78.96	97.29 ± 7.77	49.52	
NAH8524	0.40	15696 ± 73	4392 ± 23	57 ± 5	26 ± 55	9.578 ± 3.424	2.922918 ± 0.232816	81.78	87.46 ± 6.80	73.84	
NAH8526	0.45	60681 ± 163	18292 ± 48	221 ± 5	76 ± 60	15.547 ± 3.366	3.063436 ± 0.054959	92.34	91.57 ± 1.60	103.97	
NAH8528	0.50	181815 ± 430	58224 ± 83	710 ± 11	265 ± 62	4.953 ± 3.057	3.097124 ± 0.015703	99.18	92.55 ± 0.46	94.47	
NAH8530	0.58	112618 ± 274	35927 ± 68	433 ± 10	125 ± 61	1.595 ± 4.205	3.121146 ± 0.034955	99.57	93.25 ± 1.02	123.11	YES
NAH8532	0.8	230096 ± 544	73291 ± 183	893 ± 12	298 ± 70	1.561 ± 3.713	3.132938 ± 0.015167	99.79	93.59 ± 0.44	105.61	YES
NAH8534	2	150313 ± 374	47766 ± 112	590 ± 11	178 ± 56	1.466 ± 3.606	3.137463 ± 0.022567	99.70	93.72 ± 0.66	115.38	YES
NAH8537	13	54878 ± 153	16240 ± 46	196 ± 6	67 ± 66	12.809 ± 3.144	3.143602 ± 0.057817	93.03	93.90 ± 1.68	103.70	YES
NAH8540	20	3970 ± 51	318 ± 10	6 ± 3	18 ± 63	8.706 ± 3.188	4.310259 ± 2.999697	34.56	127.56 ± 85.75	7.81	YES

Plateau age (8 of 9): **93.60 ± 0.34** **MSWD: 0.34**
Inverse isochron age (8 of 9): **93.57 ± 0.70**
$(^{40}Ar/^{36}Ar)_{trapped}$ intercept: **325 ± 100**
Integrated age (9 of 9): **93.20 ± 0.35**

Sample: **NC-D**
Material: **sanidine**

File	Laser Power (%)	$^{40}Ar \pm 2\sigma_{40}$ (cps) (cps)	$^{39}Ar \pm 2\sigma_{39}$ (cps) (cps)	$^{38}Ar \pm 2\sigma_{38}$ (cps) (cps)	$^{37}Ar \pm 2\sigma_{37}$ (cps) (cps)	$^{36}Ar \pm 2\sigma_{36}$ (cps) (cps)	$^{40}Ar^*/^{39}Ar_K$ ± 2σ	$\%^{40}Ar^*$	Age (Ma) ± 2σ (Ma)	K/Ca	Included in plateau
NAH8543	0.33	24815 ± 94	6063 ± 28	72 ± 4	5 ± 48	11.455 ± 3.621	3.528353 ± 0.178332	86.21	105.07 ± 5.16	577.40	
NAH8546	0.4	59078 ± 159	18451 ± 54	223 ± 5	64 ± 74	2.572 ± 3.491	3.160037 ± 0.056504	98.69	94.38 ± 1.64	123.24	YES
NAH8548	0.45	53821 ± 154	17061 ± 45	205 ± 5	50 ± 46	1.289 ± 3.135	3.131718 ± 0.054872	99.28	93.56 ± 1.60	146.73	YES
NAH8550	0.5	114366 ± 297	36339 ± 80	444 ± 10	110 ± 57	2.206 ± 3.296	3.128821 ± 0.027104	99.41	93.47 ± 0.79	141.46	YES
NAH8552	0.58	283321 ± 663	89805 ± 154	1085 ± 16	410 ± 68	5.643 ± 4.199	3.135911 ± 0.013990	99.40	93.68 ± 0.41	94.19	YES
NAH8554	0.8	295993 ± 685	93749 ± 162	1131 ± 15	359 ± 77	3.201 ± 4.014	3.146866 ± 0.012817	99.67	94.00 ± 0.37	112.37	YES
NAH8556	2	305270 ± 715	96333 ± 122	1154 ± 14	391 ± 77	6.497 ± 3.407	3.148558 ± 0.010594	99.36	94.05 ± 0.31	105.86	YES
NAH8559	13	460752 ± 916	144074 ± 207	1745 ± 20	566 ± 74	13.585 ± 4.629	3.169649 ± 0.009624	99.11	94.66 ± 0.28	109.40	
NAH8562	20	1980 ± 50	94 ± 7	1 ± 3	7 ± 41	5.340 ± 3.073	4.112994 ± 9.847965	19.51	121.91 ± 282.39	5.68	

Plateau age (6 of 9): **93.91 ± 0.20** **MSWD: 0.81**
Inverse isochron age (6 of 9): **93.55 ± 0.04**
$(^{40}Ar/^{36}Ar)_{trapped}$ intercept: **527 ± 1000**
Integrated age (9 of 9): **94.24 ± 0.19**

Sample: **NC-D**
Material: **sanidine**

File	Laser Power (%)	$^{40}Ar \pm 2\sigma_{40}$ (cps) (cps)	$^{39}Ar \pm 2\sigma_{39}$ (cps) (cps)	$^{38}Ar \pm 2\sigma_{38}$ (cps) (cps)	$^{37}Ar \pm 2\sigma_{37}$ (cps) (cps)	$^{36}Ar \pm 2\sigma_{36}$ (cps) (cps)	$^{40}Ar^*/^{39}Ar_K$ ± 2σ	$\%^{40}Ar^*$	Age (Ma) ± 2σ (Ma)	K/Ca	Included in plateau
NAH8565	0.33	33433 ± 103	9249 ± 39	105 ± 4	36 ± 60	10.659 ± 3.026	3.270510 ± 0.097703	90.47	97.59 ± 2.84	109.75	
NAH8568	0.4	55647 ± 147	17375 ± 50	213 ± 6	55 ± 68	0.116 ± 3.071	3.200371 ± 0.052791	99.93	95.55 ± 1.54	135.44	
NAH8570	0.45	111698 ± 271	35546 ± 66	427 ± 8	153 ± 64	2.993 ± 3.218	3.117012 ± 0.027045	99.19	93.13 ± 0.79	99.99	YES
NAH8572	0.5	108950 ± 263	35008 ± 72	423 ± 8	141 ± 68	0.061 ± 3.137	3.111382 ± 0.026769	99.98	92.96 ± 0.78	106.99	YES
NAH8574	0.58	75549 ± 194	24205 ± 56	294 ± 7	106 ± 40	0.928 ± 3.085	3.109596 ± 0.038065	99.63	92.91 ± 1.11	97.76	YES
NAH8576	0.8	276475 ± 625	88163 ± 129	1075 ± 12	337 ± 83	0.340 ± 3.272	3.134588 ± 0.011114	99.96	93.64 ± 0.32	112.64	YES
NAH8578	2	285052 ± 654	90710 ± 130	1109 ± 15	351 ± 56	4.112 ± 3.383	3.128700 ± 0.011167	99.56	93.47 ± 0.33	111.19	YES
NAH8581	9	109019 ± 278	33965 ± 72	404 ± 7	149 ± 52	7.375 ± 3.049	3.144698 ± 0.026825	97.97	93.93 ± 0.78	97.72	YES
NAH8584	16	13424 ± 67	2861 ± 23	35 ± 4	9 ± 67	13.812 ± 3.370	3.250377 ± 0.351903	69.28	97.01 ± 10.23	134.81	YES

Plateau age (7 of 9): **93.49 ± 0.20** **MSWD: 1.07**
Inverse isochron age (7 of 9): **93.46 ± 0.48**
$(^{40}Ar/^{36}Ar)_{trapped}$ intercept: **332 ± 100**
Integrated age (9 of 9): **93.68 ± 0.25**

Sample: **NC-D**
Material: **sanidine**

File	Laser Power (%)	$^{40}Ar \pm 2\sigma_{40}$ (cps) (cps)	$^{39}Ar \pm 2\sigma_{39}$ (cps) (cps)	$^{38}Ar \pm 2\sigma_{38}$ (cps) (cps)	$^{37}Ar \pm 2\sigma_{37}$ (cps) (cps)	$^{36}Ar \pm 2\sigma_{36}$ (cps) (cps)	$^{40}Ar^*/^{39}Ar_K$ ± 2σ	$\%^{40}Ar^*$	Age (Ma) ± 2σ (Ma)	K/Ca	Included in plateau
NAH8587	0.33	26414 ± 91	7478 ± 32	87 ± 5	60 ± 65	6.185 ± 2.966	3.285216 ± 0.118426	93.01	98.02 ± 3.44	53.51	
NAH8590	0.4	42983 ± 123	13546 ± 39	168 ± 5	57 ± 56	2.350 ± 2.960	3.121057 ± 0.065262	98.36	93.25 ± 1.90	102.03	YES
NAH8592	0.45	83449 ± 214	26762 ± 63	323 ± 7	58 ± 57	0.722 ± 2.851	3.109833 ± 0.031830	99.73	92.92 ± 0.93	197.01	YES
NAH8594	0.5	182119 ± 451	58208 ± 98	720 ± 12	178 ± 46	2.298 ± 3.248	3.116712 ± 0.016689	99.61	93.12 ± 0.49	140.30	YES
NAH8596	0.58	164927 ± 375	52823 ± 99	638 ± 12	159 ± 55	0.266 ± 3.217	3.120437 ± 0.018208	99.94	93.23 ± 0.53	142.94	YES
NAH8598	0.8	244540 ± 558	77977 ± 133	959 ± 13	231 ± 68	1.151 ± 3.458	3.131367 ± 0.013270	99.85	93.55 ± 0.39	145.18	YES
NAH8600	2	78031 ± 193	24662 ± 57	289 ± 7	92 ± 49	2.389 ± 2.982	3.134768 ± 0.036117	99.08	93.64 ± 1.05	115.12	YES
NAH8603	9	29310 ± 94	8403 ± 33	103 ± 4	54 ± 80	10.907 ± 2.908	3.100367 ± 0.103336	88.89	92.64 ± 3.01	67.37	YES
NAH8606	16	5224 ± 48	359 ± 8	7 ± 4	4 ± 71	14.404 ± 3.350	2.568495 ± 2.796414	17.67	77.08 ± 82.18	41.37	YES

Plateau age (8 of 9): **93.32 ± 0.25** **MSWD: 0.52**
Inverse isochron age (8 of 9): **93.35 ± 0.47**
$(^{40}Ar/^{36}Ar)_{trapped}$ intercept: **285 ± 79**
Integrated age (9 of 9): **93.40 ± 0.30**

Sample: **NC-D**
Material: **sanidine**

File	Laser Power (%)	$^{40}Ar \pm 2\sigma_{40}$ (cps)	$^{39}Ar \pm 2\sigma_{39}$ (cps)	$^{38}Ar \pm 2\sigma_{38}$ (cps)	$^{37}Ar \pm 2\sigma_{37}$ (cps)	$^{36}Ar \pm 2\sigma_{36}$ (cps)	$^{40}Ar^*/^{39}Ar_K \pm 2\sigma$	$\%^{40}Ar^*$	Age (Ma) ± 2σ (Ma)	K/Ca	Included in plateau
NAH8609	0.35	59028 ± 162	17527 ± 47	211 ± 6	89 ± 75	8.588 ± 2.788	3.221358 ± 0.047513	95.65	96.16 ± 1.38	85.09	
NAH8612	0.42	181061 ± 406	57367 ± 82	693 ± 9	256 ± 67	5.823 ± 3.072	3.125699 ± 0.016009	99.03	93.38 ± 0.47	96.25	YES
NAH8614	0.47	237393 ± 535	75775 ± 146	924 ± 15	331 ± 47	4.426 ± 3.469	3.115260 ± 0.013699	99.44	93.08 ± 0.40	98.57	YES
NAH8616	0.52	237617 ± 525	75851 ± 110	929 ± 10	322 ± 60	1.705 ± 2.833	3.125765 ± 0.011184	99.78	93.38 ± 0.33	101.19	YES
NAH8618	0.6	193954 ± 435	61999 ± 94	752 ± 12	291 ± 68	0.296 ± 3.286	3.126729 ± 0.015846	99.95	93.41 ± 0.46	91.60	YES
NAH8620	0.8	272656 ± 600	86904 ± 112	1052 ± 13	388 ± 53	1.015 ± 3.201	3.133760 ± 0.011027	99.88	93.62 ± 0.32	96.38	YES
NAH8622	2	53253 ± 158	16672 ± 44	198 ± 6	86 ± 70	2.237 ± 2.860	3.153901 ± 0.051224	98.74	94.20 ± 1.49	83.67	YES
NAH8624	9	24224 ± 83	4683 ± 29	61 ± 4	7 ± 46	16.679 ± 3.336	4.109347 ± 0.212813	79.44	121.81 ± 6.10	269.07	

Plateau age (6 of 8): **93.41 ± 0.17** **MSWD: 1.12**
Inverse isochron age (6 of 8): **93.40 ± 2.10**
$(^{40}Ar/^{36}Ar)_{trapped}$ intercept: **288 ± 310**
Integrated age (8 of 8): **93.87 ± 0.19**

Sample: **NC-D**
Material: **sanidine**

File	Laser Power (%)	$^{40}Ar \pm 2\sigma_{40}$ (cps)	$^{39}Ar \pm 2\sigma_{39}$ (cps)	$^{38}Ar \pm 2\sigma_{38}$ (cps)	$^{37}Ar \pm 2\sigma_{37}$ (cps)	$^{36}Ar \pm 2\sigma_{36}$ (cps)	$^{40}Ar^*/^{39}Ar_K \pm 2\sigma$	$\%^{40}Ar^*$	Age (Ma) ± 2σ (Ma)	K/Ca	Included in plateau
NAH8630	0.35	92746 ± 214	27313 ± 65	332 ± 7	97 ± 56	20.851 ± 3.305	3.167531 ± 0.036149	93.28	94.60 ± 1.05	121.28	
NAH8633	0.42	172908 ± 353	54794 ± 76	670 ± 8	248 ± 72	6.590 ± 2.823	3.119518 ± 0.015404	98.86	93.20 ± 0.45	94.88	YES
NAH8635	0.47	153130 ± 330	48879 ± 86	595 ± 9	229 ± 52	2.889 ± 3.061	3.115036 ± 0.018716	99.43	93.07 ± 0.55	91.87	YES
NAH8637	0.52	135693 ± 291	43395 ± 75	518 ± 8	210 ± 54	0.410 ± 2.966	3.123982 ± 0.020424	99.90	93.33 ± 0.59	89.01	YES
NAH8639	0.6	181609 ± 436	57551 ± 139	702 ± 11	253 ± 71	2.600 ± 4.119	3.141941 ± 0.021394	99.57	93.85 ± 0.62	97.71	YES
NAH8641	0.8	116631 ± 258	37178 ± 79	450 ± 7	171 ± 59	2.448 ± 2.832	3.117237 ± 0.022766	99.37	93.13 ± 0.66	93.52	YES
NAH8643	2	178494 ± 391	56735 ± 82	679 ± 9	250 ± 42	3.988 ± 2.992	3.124926 ± 0.015766	99.33	93.36 ± 0.46	97.44	YES
NAH8645	9	131014 ± 308	41375 ± 73	499 ± 10	203 ± 49	6.730 ± 3.110	3.117802 ± 0.022462	98.46	93.15 ± 0.65	87.71	YES
NAH8648	16	1282 ± 47	93 ± 8	3 ± 5	4 ± 43	3.720 ± 2.917	1.843102 ± 9.408837	13.39	55.64 ± 279.75	9.80	YES

Plateau age (8 of 9): **93.29 ± 0.21** **MSWD: 0.67**
Inverse isochron age (8 of 9): **93.40 ± 1.50**
$(^{40}Ar/^{36}Ar)_{trapped}$ intercept: **261 ± 210**
Integrated age (9 of 9): **93.41 ± 0.22**

Sample: **NC-D**
Material: **sanidine**

File	Laser Power (%)	$^{40}Ar \pm 2\sigma_{40}$ (cps)	$^{39}Ar \pm 2\sigma_{39}$ (cps)	$^{38}Ar \pm 2\sigma_{38}$ (cps)	$^{37}Ar \pm 2\sigma_{37}$ (cps)	$^{36}Ar \pm 2\sigma_{36}$ (cps)	$^{40}Ar^*/^{39}Ar_K \pm 2\sigma$	$\%^{40}Ar^*$	Age (Ma) ± 2σ (Ma)	K/Ca	Included in plateau
NAH8651	0.35	97930 ± 234	30274 ± 73	358 ± 7	128 ± 49	7.487 ± 3.046	3.160769 ± 0.030057	97.71	94.40 ± 0.87	101.64	
NAH8654	0.42	149426 ± 358	47405 ± 75	570 ± 8	239 ± 68	5.913 ± 2.959	3.114713 ± 0.018660	98.81	93.06 ± 0.54	85.26	YES
NAH8656	0.47	152527 ± 342	48606 ± 76	597 ± 8	240 ± 51	3.790 ± 2.659	3.114645 ± 0.016356	99.25	93.06 ± 0.48	87.22	YES
NAH8658	0.52	151932 ± 336	48457 ± 74	588 ± 9	238 ± 51	2.868 ± 2.955	3.117571 ± 0.018230	99.43	93.14 ± 0.53	87.61	YES
NAH8660	0.6	99147 ± 226	31532 ± 62	381 ± 8	139 ± 42	1.492 ± 2.666	3.130048 ± 0.025258	99.54	93.51 ± 0.74	97.69	YES
NAH8662	0.8	71958 ± 175	22983 ± 55	283 ± 7	90 ± 45	1.608 ± 3.135	3.109766 ± 0.040745	99.33	92.92 ± 1.19	109.99	YES
NAH8664	2	88890 ± 199	28265 ± 59	343 ± 7	127 ± 54	2.657 ± 2.911	3.116670 ± 0.030763	99.10	93.12 ± 0.90	96.03	YES
NAH8667	9	114285 ± 269	35742 ± 69	437 ± 8	172 ± 64	6.766 ± 3.020	3.140819 ± 0.025243	98.23	93.82 ± 0.74	89.17	YES
NAH8670	16	1136 ± 49	39 ± 7	1 ± 4	3 ± 55	3.257 ± 2.809	4.178970 ± 21.83716	14.44	123.80 ± 625.54	6.41	YES

Plateau age (8 of 9): **93.21 ± 0.25** **MSWD: 0.64**
Inverse isochron age (8 of 9): **92.90 ± 2.90**
$(^{40}Ar/^{36}Ar)_{trapped}$ intercept: **405 ± 330**
Integrated age (9 of 9): **93.35 ± 0.26**

Sample: **NC-D**
Material: **sanidine**

File	Laser Power (%)	$^{40}Ar \pm 2\sigma_{40}$ (cps)	$^{39}Ar \pm 2\sigma_{39}$ (cps)	$^{38}Ar \pm 2\sigma_{38}$ (cps)	$^{37}Ar \pm 2\sigma_{37}$ (cps)	$^{36}Ar \pm 2\sigma_{36}$ (cps)	$^{40}Ar^*/^{39}Ar_K$	± 2σ	%$^{40}Ar^*$	Age (Ma)	± 2σ (Ma)	K/Ca	Included in plateau
NAH8673	0.35	58838 ± 179	17979 ± 51	217 ± 7	84 ± 65	7.663 ± 3.257	3.145111	± 0.054108	96.11	93.95	± 1.58	91.94	YES
NAH8676	0.42	128021 ± 313	36165 ± 72	449 ± 8	256 ± 60	49.787 ± 4.061	3.128958	± 0.033550	88.39	93.48	± 0.98	60.80	YES
NAH8678	0.47	262270 ± 639	83798 ± 134	1016 ± 13	487 ± 72	0.352 ± 3.048	3.128465	± 0.010899	99.96	93.46	± 0.32	73.93	YES
NAH8680	0.52	153674 ± 383	48871 ± 85	594 ± 9	300 ± 49	2.534 ± 3.191	3.128993	± 0.019516	99.51	93.48	± 0.57	70.04	YES
NAH8682	0.6	70144 ± 192	22348 ± 52	266 ± 6	116 ± 60	1.574 ± 2.701	3.117511	± 0.036106	99.33	93.14	± 1.05	83.08	YES
NAH8684	0.8	68456 ± 183	21634 ± 58	263 ± 6	184 ± 55	2.120 ± 2.951	3.135218	± 0.040744	99.08	93.66	± 1.19	50.68	YES
NAH8686	2	41667 ± 130	13174 ± 38	156 ± 7	40 ± 45	2.767 ± 3.074	3.099753	± 0.069682	98.01	92.62	± 2.03	140.92	YES
NAH8689	9	64815 ± 203	20060 ± 72	237 ± 7	103 ± 62	0.314 ± 4.020	3.226283	± 0.059854	99.85	96.31	± 1.74	83.40	
NAH8692	16	1607 ± 48	104 ± 8	3 ± 3	6 ± 66	6.540 ± 3.127	-3.300017	± 9.04156	-21.44	-104.05	± 293.34	7.73	

Plateau age (7 of 9): **93.46 ± 0.25** **MSWD: 0.26**
Inverse isochron age (7 of 9): **93.47 ± 0.49**
$(^{40}Ar/^{36}Ar)_{trapped}$ intercept: **300 ± 41**
Integrated age (9 of 9): **93.58 ± 0.33**

Sample: **NC-D**
Material: **sanidine**

File	Laser Power (%)	$^{40}Ar \pm 2\sigma_{40}$ (cps)	$^{39}Ar \pm 2\sigma_{39}$ (cps)	$^{38}Ar \pm 2\sigma_{38}$ (cps)	$^{37}Ar \pm 2\sigma_{37}$ (cps)	$^{36}Ar \pm 2\sigma_{36}$ (cps)	$^{40}Ar^*/^{39}Ar_K$	± 2σ	%$^{40}Ar^*$	Age (Ma)	± 2σ (Ma)	K/Ca	Included in plateau
NAH8695	0.35	142452 ± 353	44096 ± 85	524 ± 8	248 ± 63	7.964 ± 3.123	3.176499	± 0.021170	98.33	94.86	± 0.62	76.47	
NAH8698	0.42	303030 ± 690	95918 ± 96	1164 ± 11	514 ± 66	6.726 ± 3.063	3.138204	± 0.009568	99.33	93.74	± 0.28	80.32	YES
NAH8700	0.47	409280 ± 902	130051 ± 138	1579 ± 14	687 ± 95	8.023 ± 3.140	3.128544	± 0.007251	99.41	93.46	± 0.21	81.45	YES
NAH8702	0.52	111595 ± 275	35364 ± 67	425 ± 9	164 ± 63	2.764 ± 2.880	3.132142	± 0.024332	99.26	93.57	± 0.71	92.94	YES
NAH8704	0.6	85012 ± 220	26991 ± 53	321 ± 7	120 ± 47	1.124 ± 2.907	3.137066	± 0.032178	99.60	93.71	± 0.94	96.33	YES
NAH8706	0.8	33008 ± 111	10298 ± 39	125 ± 5	55 ± 39	1.373 ± 3.133	3.165366	± 0.090837	98.75	94.54	± 2.64	80.10	YES
NAH8708	2	24816 ± 81	7598 ± 35	91 ± 5	45 ± 74	2.975 ± 2.881	3.149337	± 0.113227	96.42	94.07	± 3.30	72.36	YES
NAH8711	9	19737 ± 78	5783 ± 29	72 ± 4	63 ± 53	3.600 ± 3.101	3.227229	± 0.160092	94.56	96.34	± 4.66	39.42	YES

Plateau age (7 of 8): **93.58 ± 0.17** **MSWD: 0.78**
Inverse isochron age (7 of 8): **93.30 ± 8.30**
$(^{40}Ar/^{36}Ar)_{trapped}$ intercept: **471 ± 440**
Integrated age (8 of 8): **93.83 ± 0.21**

Sample: **NC-D**
Material: **sanidine**

File	Laser Power (%)	$^{40}Ar \pm 2\sigma_{40}$ (cps)	$^{39}Ar \pm 2\sigma_{39}$ (cps)	$^{38}Ar \pm 2\sigma_{38}$ (cps)	$^{37}Ar \pm 2\sigma_{37}$ (cps)	$^{36}Ar \pm 2\sigma_{36}$ (cps)	$^{40}Ar^*/^{39}Ar_K$	± 2σ	%$^{40}Ar^*$	Age (Ma)	± 2σ (Ma)	K/Ca	Included in plateau
NAH8714	0.35	66833 ± 171	19938 ± 48	236 ± 6	96 ± 55	8.504 ± 3.198	3.224540	± 0.047906	96.20	96.26	± 1.39	89.09	
NAH8717	0.42	108219 ± 266	34225 ± 76	414 ± 8	132 ± 72	4.833 ± 3.194	3.119616	± 0.027879	98.66	93.20	± 0.81	111.63	YES
NAH8719	0.47	145956 ± 344	46596 ± 82	559 ± 9	214 ± 57	1.858 ± 2.759	3.120321	± 0.017701	99.61	93.22	± 0.52	93.41	YES
NAH8721	0.52	317038 ± 732	100886 ± 180	1230 ± 16	414 ± 58	3.738 ± 3.534	3.131281	± 0.010498	99.64	93.54	± 0.31	104.79	YES
NAH8723	0.6	241762 ± 548	77339 ± 117	933 ± 12	354 ± 54	0.787 ± 2.775	3.122784	± 0.010749	99.90	93.30	± 0.31	93.94	YES
NAH8725	0.8	282616 ± 664	89882 ± 166	1074 ± 16	420 ± 75	5.057 ± 3.443	3.127333	± 0.011477	99.46	93.43	± 0.33	91.91	YES
NAH8727	2	227502 ± 591	71868 ± 157	854 ± 15	309 ± 60	6.532 ± 3.693	3.138206	± 0.015379	99.14	93.74	± 0.45	100.16	YES
NAH8730	9	89270 ± 232	27613 ± 63	332 ± 7	131 ± 89	2.072 ± 2.922	3.210328	± 0.031617	99.30	95.84	± 0.92	90.71	

Plateau age (6 of 8): **93.44 ± 0.16** **MSWD: 0.84**
Inverse isochron age (6 of 8): **93.30 ± 2.80**
$(^{40}Ar/^{36}Ar)_{trapped}$ intercept: **396 ± 350**
Integrated age (8 of 8): **93.71 ± 0.18**

Sample: **NC-D**
Material: **sanidine**

File	Laser Power (%)	$^{40}Ar \pm 2\sigma_{40}$ (cps)	$^{39}Ar \pm 2\sigma_{39}$ (cps)	$^{38}Ar \pm 2\sigma_{38}$ (cps)	$^{37}Ar \pm 2\sigma_{37}$ (cps)	$^{36}Ar \pm 2\sigma_{36}$ (cps)	$^{40}Ar^*/^{39}Ar_K$ ± 2σ	$\%^{40}Ar^*$	Age (Ma) ± 2σ (Ma)	K/Ca	Included in plateau
NAH8736	0.35	36571 ± 102	10605 ± 39	126 ± 5	32 ± 73	4.862 ± 2.992	3.311401 ± 0.084236	96.02	98.78 ± 2.45	143.14	
NAH8739	0.42	29870 ± 93	9287 ± 33	112 ± 5	33 ± 56	1.473 ± 3.078	3.168800 ± 0.098956	98.52	94.64 ± 2.88	120.19	
NAH8741	0.47	25794 ± 98	8132 ± 36	102 ± 5	38 ± 76	0.285 ± 2.982	3.161457 ± 0.109497	99.67	94.42 ± 3.19	91.97	
NAH8743	0.52	61398 ± 165	15165 ± 46	193 ± 6	87 ± 65	36.992 ± 3.937	3.320342 ± 0.077555	82.01	99.04 ± 2.25	74.54	
NAH8745	0.6	120838 ± 280	38745 ± 68	472 ± 9	194 ± 68	2.976 ± 3.032	3.095719 ± 0.023386	99.26	92.51 ± 0.68	85.66	
NAH8747	0.8	364970 ± 778	116804 ± 121	1418 ± 13	576 ± 68	1.727 ± 2.925	3.120078 ± 0.007516	99.85	93.22 ± 0.22	87.15	
NAH8749	2	249940 ± 580	79547 ± 130	961 ± 11	323 ± 60	2.107 ± 3.260	3.133905 ± 0.012270	99.74	93.62 ± 0.36	105.96	
NAH8752	9	116005 ± 272	36168 ± 73	437 ± 8	178 ± 61	8.570 ± 2.719	3.136492 ± 0.022467	97.79	93.69 ± 0.65	87.56	
NAH8755	16	6728 ± 61	1584 ± 17	20 ± 3	4 ± 76	6.594 ± 3.187	3.003233 ± 0.600780	70.73	89.81 ± 17.53	156.68	

no plateau

Integrated age (8 of 8): **93.81 ± 0.27**

Sample: **NC-D**
Material: **sanidine**

File	Laser Power (%)	$^{40}Ar \pm 2\sigma_{40}$ (cps)	$^{39}Ar \pm 2\sigma_{39}$ (cps)	$^{38}Ar \pm 2\sigma_{38}$ (cps)	$^{37}Ar \pm 2\sigma_{37}$ (cps)	$^{36}Ar \pm 2\sigma_{36}$ (cps)	$^{40}Ar^*/^{39}Ar_K$ ± 2σ	$\%^{40}Ar^*$	Age (Ma) ± 2σ (Ma)	K/Ca	Included in plateau
NAH8758	0.4	142258 ± 337	43625 ± 79	525 ± 8	169 ± 72	13.923 ± 3.714	3.165407 ± 0.025432	97.07	94.54 ± 0.74	111.28	
NAH8761	0.46	182779 ± 426	57682 ± 97	705 ± 10	228 ± 49	5.547 ± 2.715	3.139821 ± 0.014084	99.09	93.79 ± 0.41	108.93	YES
NAH8763	0.52	227176 ± 531	71875 ± 151	865 ± 12	313 ± 54	6.491 ± 4.078	3.133581 ± 0.016968	99.14	93.61 ± 0.49	98.79	YES
NAH8765	0.6	142906 ± 350	45251 ± 96	542 ± 12	254 ± 60	5.374 ± 3.191	3.122521 ± 0.021082	98.87	93.29 ± 0.61	76.61	YES
NAH8767	0.8	79730 ± 216	25193 ± 69	309 ± 8	157 ± 55	1.301 ± 3.276	3.149291 ± 0.038842	99.51	94.07 ± 1.13	69.17	YES
NAH8769	1.5	35456 ± 128	11084 ± 50	131 ± 5	74 ± 57	0.247 ± 2.897	3.192190 ± 0.078042	99.79	95.32 ± 2.27	64.73	YES
NAH8771	5	41432 ± 138	12931 ± 48	156 ± 7	81 ± 45	4.430 ± 3.005	3.101673 ± 0.069388	96.81	92.68 ± 2.02	68.75	YES
NAH8774	15	4225 ± 54	841 ± 14	12 ± 4	22 ± 45	5.193 ± 3.289	3.182512 ± 1.168346	63.33	95.03 ± 34.00	16.40	YES

Plateau age (7 of 8): **93.66 ± 0.27** **MSWD: 0.92**
Inverse isochron age (7 of 8): **93.80 ± 1.80**
$(^{40}Ar/^{36}Ar)_{trapped}$ intercept: **268 ± 210**
Integrated age (8 of 8): **93.82 ± 0.30**

The isotope values in this table have been corrected for system blanks, source mass bias, detector efficiency, and decay of 37Ar and 39Ar

Instrument: Noblesse 5-collector mass spectrometer (Jicha et al., 2016)
Standard: Fish Canyon sanidine
Standard age (Ma): 28.201 ± 0.046 Kuiper et al. (2008)
J-value: 0.01674374 ± 0.00000348 (1σ) *J value is the same for all 3 samples because they were in the same, small irradiation position

Atmospheric argon ratios

$^{40}Ar/^{36}Ar$	298.56 ± 0.31	Lee et al. (2006)
$^{38}Ar/^{36}Ar$	0.1885 ± 0.0003	Lee et al. (2006)

Interfering isotope production ratios

$(^{40}Ar/^{39}Ar)_K$	0.00054 ± 0.00014	Jicha & Brown (2014)
$(^{38}Ar/^{39}Ar)_K$	0.01210 ± 0.00002	Jicha & Brown (2014)
$(^{39}Ar/^{37}Ar)_{Ca}$	0.000695 ± 0.00001	Renne et al. (2013)
$(^{38}Ar/^{37}Ar)_{Ca}$	0.0000196 ± 0.000001	Renne et al. (2013)
$(^{36}Ar/^{37}Ar)_{Ca}$	0.000265 ± 0.00002	Renne et al. (2013)

Decay constants

l_{40Ar}	$(0.580 \pm 0.014) \times 10^{-10}$ a^{-1}	Min et al. (2000)
l_{B^-}	$(4.884 \pm 0.099) \times 10^{-10}$ a^{-1}	Min et al. (2000)
^{39}Ar	0.000007068 1/days	
^{37}Ar	0.01975 1/days	
^{36}Cl	6.308E-09 1/days	
$^{36}Cl/^{38}Cl$	263	Renne et al. (2008)

Table S5. Complete Ar data for samples 90-O-34 and K-07-01C

Sample: 90-0-34 **Identifier: UW144:A7**
Material: Sanidine **Location: Lohali Point, Arizona (Bentonite D, bed BM-17 of Kirkland, 1991)**

N	Power %	Age (Ma)	±1σ (Ma)	K/Ca	±1σ	%^{40}Ar (%)	^{40}Ar*/^{39}Ar$_K$	Corrected[1] ^{40}Ar (cps)	±1σ	^{39}Ar (cps)	±1σ	^{38}Ar (cps)	±1σ
01A	18	93.81	0.14	62.542	5.075	97.671	3.1405759	418921.136950	356.1629325	130145.1670338	74.8067692	1547.4557933	6.7349795
02A	18	93.64	0.10	55.44	2.547	99.499	3.1347307	622540.1641816	467.886350	197388.9027605	88.6475377	2379.7267091	8.7362051
03A	18	93.70	0.11	76.102	6.719	99.368	3.136620	563997.8448798	448.2506036	178484.8609507	88.0428672	2149.0256725	7.5075358
X 04A	18	94.23	0.13	63.779	6.381	99.328	3.1547135	384898.1256855	313.0876195	121058.2983684	71.3829374	1463.5563735	6.6105167
05A	18	93.71	0.12	54.71	3.061	98.988	3.1369215	485473.9846989	403.9182577	153032.101222	81.3769961	1829.679860	7.4885408
X 06A	18	94.32	0.14	86.39	11.525	99.262	3.1581111	328936.1724764	261.2781014	103277.5937138	72.6157782	1229.4763259	6.5935572
07A	18	93.78	0.11	71.353	4.911	99.352	3.1395242	576124.4609781	463.6368004	182123.5045486	90.8284133	2190.3374136	8.2442961
08A	18	94.02	0.16	64.907	9.962	99.108	3.1477844	254554.5600423	220.1422805	80061.7251899	57.2901189	959.3726819	5.124715
09A	18	93.91	0.11	70.043	5.399	99.589	3.1438745	462911.420707	379.2176065	146481.6170778	81.4098396	1762.9776588	8.0860984
10A	18	93.92	0.11	64.464	3.781	99.329	3.1442837	602144.2333563	488.1211629	190016.8042753	100.9981837	2313.7996718	7.4896101
12A	18	93.81	0.10	63.512	4.71	99.391	3.1404303	561165.6408577	447.7657368	177412.9606134	89.8719836	2149.0507983	7.8806772
13A	18	93.84	0.14	53.52	5.04	99.384	3.1415433	333558.8294249	270.5136597	105410.8536514	56.260146	1277.285975	6.1314673
14A	18	93.91	0.11	80.902	6.563	99.333	3.1438118	524463.5286827	412.4031364	165534.509287	81.048465	1994.8233963	8.2303527
15A	18	93.96	0.11	61.912	3.758	99.357	3.1454572	609233.3798983	517.4421945	192237.6460843	103.607522	2312.0632115	8.3209204
16A	18	93.78	0.15	68.964	5.004	98.591	3.1392786	540050.2359153	440.6097436	169425.4255217	90.3112755	2031.4730146	8.0274173
17A	18	93.76	0.13	63.822	5.505	98.32	3.1386476	427221.970802	350.0750643	133687.5111649	72.8567331	1618.0511637	7.738740
18A	18	94.00	0.11	80.196	6.277	98.855	3.1469514	545020.6139596	450.9205241	171024.5115775	93.1506685	2055.1843922	7.6084918
19A	18	93.66	0.12	42.888	1.667	99.205	3.1354075	598252.579758	542.7187474	189087.9160494	86.6098862	2266.0843734	8.1511638
20A	18	93.95	0.12	62.982	4.494	99.190	3.1451141	452942.4967836	363.4258315	142696.0025204	81.8428718	1716.8588597	7.441658
21A	18	93.76	0.11	71.611	5.064	99.488	3.1386024	496888.7895786	406.2567764	157337.4731141	84.1700917	1891.7476887	7.3860825
22A	18	93.91	0.13	63.489	5.544	99.305	3.143837	381806.9464429	304.8778172	120474.0101145	74.835830	1454.5555144	6.612253
23A	18	93.84	0.19	63.493	8.309	99.537	3.1414042	254304.2338196	221.2555783	80491.8626434	56.5439593	960.5572773	5.4833227
25A	18	93.63	0.13	50.284	3.266	99.098	3.134181	436345.5039049	376.660861	137819.5036418	84.447869	1656.6745175	7.3787719
X 26A	18	94.26	0.12	73.665	6.846	99.556	3.1557626	449537.2084011	372.5718139	141666.4131494	79.8382989	1693.2734946	7.2946964
27A	18	93.59	0.11	71.333	4.987	99.386	3.132804	564545.9450149	465.8596476	178906.8620038	87.9456924	2155.8340045	7.7881737
28A	18	93.84	0.12	67.254	5.42	99.004	3.1415014	469324.177496	364.7117679	147748.6798711	71.7641426	1790.5069416	7.3092983
29A	18	93.61	0.12	79.60	7.335	99.288	3.1335549	450627.7950318	358.4335088	142630.4817703	81.0985488	1719.7492734	7.5327949
Weighted mean K/Ca ±2σ				**57.667**	**4.617**								
Weighted mean Age ±2σ		**93.8**	**0.07**	**n=24/27**		**MSWD=1.151**							

N	^{37}Ar (cps)	±1σ	^{36}Ar (cps)	±1σ	RunDate	Δt[3] (days)	J	±1σ	^{39}Ar Decay	^{37}Ar Decay	LambdaK
01A	45.974043	3.730804	30.5486259	1.5907407	04/28/19 11:42	169.849838	0.0167473	3.48313E-06	1.0010675	19.5306854	5.464E-10
02A	78.6288732	3.6126592	7.2859833	1.3208108	04/28/19 12:11	169.8698958	0.0167473	3.48313E-06	1.0010676	19.5384239	5.464E-10
03A	51.7812146	4.5714329	8.9667174	1.3290584	04/28/19 12:31	169.8838426	0.0167473	3.48313E-06	1.0010677	19.5438064	5.464E-10
X 04A	41.8899361	4.1908628	6.6917506	1.1671961	04/28/19 13:00	169.9038426	0.0167473	3.48313E-06	1.0010679	19.5515277	5.464E-10
05A	61.7152463	3.4523952	14.0013878	1.2931047	04/28/19 13:20	169.9178125	0.0167473	3.48313E-06	1.001068	19.5569229	5.464E-10
X 06A	26.3660391	3.5173262	6.3887341	1.1710919	04/28/19 13:49	169.9377431	0.0167473	3.48313E-06	1.0010681	19.5646225	5.464E-10
07A	56.2779947	3.8730542	9.4992204	1.2498407	04/28/19 14:09	169.9517593	0.0167473	3.48313E-06	1.0010682	19.5700392	5.464E-10
08A	27.1859185	4.1724575	6.2894178	1.1664211	04/28/19 14:38	169.9717361	0.0167473	3.48313E-06	1.0010684	19.5777619	5.464E-10
09A	46.0799012	3.5516412	3.9525057	1.1535316	04/28/19 14:58	169.985706	0.0167473	3.48313E-06	1.0010685	19.5831643	5.464E-10
10A	64.9221788	3.8072239	10.4372131	1.2881195	04/28/19 15:27	170.0057986	0.0167473	3.48313E-06	1.0010686	19.590937	5.464E-10
12A	61.4832037	4.5596626	8.5607913	1.1697512	04/28/19 16:16	170.0397454	0.0167473	3.48313E-06	1.0010688	19.6040761	5.464E-10
13A	43.3388309	4.0814324	5.1959899	1.3014409	04/28/19 16:36	170.0537616	0.0167473	3.48313E-06	1.0010689	19.6095037	5.464E-10
14A	45.0055087	3.6506656	8.9555452	1.2609866	04/28/19 17:05	170.0739468	0.0167473	3.48313E-06	1.0010691	19.6173227	5.464E-10
15A	68.2778274	4.1442337	9.9805061	1.1650288	04/28/19 17:25	170.0877199	0.0167473	3.48313E-06	1.0010692	19.6226597	5.464E-10
16A	54.001045	3.9181225	22.6958823	2.4397556	04/28/19 17:54	170.1076505	0.0167473	3.48313E-06	1.0010693	19.6303853	5.464E-10
17A	46.0308576	3.9700432	21.8569467	1.4270786	04/28/19 18:13	170.1214699	0.0167473	3.48313E-06	1.0010694	19.6357438	5.464E-10
18A	46.8448464	3.6667352	18.0458748	1.3225878	04/28/19 18:42	170.1416088	0.0167473	3.48313E-06	1.0010696	19.6435553	5.464E-10
19A	96.8186047	3.7632043	12.9990457	1.5530312	04/28/19 19:02	170.1553935	0.0167473	3.48313E-06	1.0010697	19.648904	5.464E-10
20A	49.7346781	3.5487128	9.9616135	1.3377032	04/28/19 19:31	170.1754167	0.0167473	3.48313E-06	1.0010698	19.6566758	5.464E-10
21A	48.2169988	3.4093572	5.9149142	1.2658167	04/28/19 19:51	170.1893287	0.0167473	3.48313E-06	1.0010699	19.6620775	5.464E-10
22A	41.6262754	3.6350178	6.9192986	1.2807529	04/28/19 20:20	170.2094329	0.0167473	3.48313E-06	1.001070	19.669886	5.464E-10
23A	27.8021141	3.6384084	2.6268067	1.5135325	04/28/19 20:40	170.2234028	0.0167473	3.48313E-06	1.0010701	19.6753138	5.464E-10
25A	60.0682351	3.9012785	10.9919902	1.4763194	04/28/19 21:29	170.2574537	0.0167473	3.48313E-06	1.0010704	19.688550	5.464E-10
X 26A	42.1303396	3.9154809	4.3298583	1.2279766	04/28/19 21:58	170.2775347	0.0167473	3.48313E-06	1.0010705	19.696360	5.464E-10
27A	54.9296029	3.8400727	8.6599414	1.2945629	04/28/19 22:18	170.291412	0.0167473	3.48313E-06	1.0010706	19.7017591	5.464E-10
28A	48.0951061	3.8756471	13.2393103	1.4488819	04/28/19 22:47	170.3115046	0.0167473	3.48313E-06	1.0010708	19.7095789	5.464E-10
29A	39.2172948	3.6139224	8.3727679	1.2469202	04/28/19 23:07	170.3254051	0.0167473	3.48313E-06	1.0010709	19.7149906	5.464E-10

N	MonitorAge	MonitorName	MonitorMaterial	(^{40}Ar/^{39}39)$_K$	±1σ	(^{38}Ar/^{39}39)$_K$	±1σ	(^{37}Ar/^{39}39)$_K$	±1σ	(^{39}Ar/^{37}37)$_{Ca}$	±1σ	(^{38}Ar/^{37}37)$_{Ca}$	±1σ	(^{36}Ar/^{37}37)$_{Ca}$	±1σ	(^{36}Ar/^{38}38)$_{Cl}$	Ca/K	Cl/K
01A	28.201	FC-2	sanidine	0.005400	0.000140	0.012100	0.000050	0.000000	0.000000	0.000695	0.000018	0.0000196	0.0000016	0.000265	0.000004	263.000000	2.320000	0.227000
02A	28.201	FC-2	sanidine	0.005400	0.000140	0.012100	0.000050	0.000000	0.000000	0.000695	0.000018	0.0000196	0.0000016	0.000265	0.000004	263.000000	2.320000	0.227000
03A	28.201	FC-2	sanidine	0.005400	0.000140	0.012100	0.000050	0.000000	0.000000	0.000695	0.000018	0.0000196	0.0000016	0.000265	0.000004	263.000000	2.320000	0.227000
X 04A	28.201	FC-2	sanidine	0.005400	0.000140	0.012100	0.000050	0.000000	0.000000	0.000695	0.000018	0.0000196	0.0000016	0.000265	0.000004	263.000000	2.320000	0.227000
05A	28.201	FC-2	sanidine	0.005400	0.000140	0.012100	0.000050	0.000000	0.000000	0.000695	0.000018	0.0000196	0.0000016	0.000265	0.000004	263.000000	2.320000	0.227000
X 06A	28.201	FC-2	sanidine	0.005400	0.000140	0.012100	0.000050	0.000000	0.000000	0.000695	0.000018	0.0000196	0.0000016	0.000265	0.000004	263.000000	2.320000	0.227000
07A	28.201	FC-2	sanidine	0.005400	0.000140	0.012100	0.000050	0.000000	0.000000	0.000695	0.000018	0.0000196	0.0000016	0.000265	0.000004	263.000000	2.320000	0.227000
08A	28.201	FC-2	sanidine	0.005400	0.000140	0.012100	0.000050	0.000000	0.000000	0.000695	0.000018	0.0000196	0.0000016	0.000265	0.000004	263.000000	2.320000	0.227000
09A	28.201	FC-2	sanidine	0.005400	0.000140	0.012100	0.000050	0.000000	0.000000	0.000695	0.000018	0.0000196	0.0000016	0.000265	0.000004	263.000000	2.320000	0.227000
10A	28.201	FC-2	sanidine	0.005400	0.000140	0.012100	0.000050	0.000000	0.000000	0.000695	0.000018	0.0000196	0.0000016	0.000265	0.000004	263.000000	2.320000	0.227000
12A	28.201	FC-2	sanidine	0.005400	0.000140	0.012100	0.000050	0.000000	0.000000	0.000695	0.000018	0.0000196	0.0000016	0.000265	0.000004	263.000000	2.320000	0.227000
13A	28.201	FC-2	sanidine	0.005400	0.000140	0.012100	0.000050	0.000000	0.000000	0.000695	0.000018	0.0000196	0.0000016	0.000265	0.000004	263.000000	2.320000	0.227000
14A	28.201	FC-2	sanidine	0.005400	0.000140	0.012100	0.000050	0.000000	0.000000	0.000695	0.000018	0.0000196	0.0000016	0.000265	0.000004	263.000000	2.320000	0.227000
15A	28.201	FC-2	sanidine	0.005400	0.000140	0.012100	0.000050	0.000000	0.000000	0.000695	0.000018	0.0000196	0.0000016	0.000265	0.000004	263.000000	2.320000	0.227000
16A	28.201	FC-2	sanidine	0.005400	0.000140	0.012100	0.000050	0.000000	0.000000	0.000695	0.000018	0.0000196	0.0000016	0.000265	0.000004	263.000000	2.320000	0.227000
17A	28.201	FC-2	sanidine	0.005400	0.000140	0.012100	0.000050	0.000000	0.000000	0.000695	0.000018	0.0000196	0.0000016	0.000265	0.000004	263.000000	2.320000	0.227000
18A	28.201	FC-2	sanidine	0.005400	0.000140	0.012100	0.000050	0.000000	0.000000	0.000695	0.000018	0.0000196	0.0000016	0.000265	0.000004	263.000000	2.320000	0.227000
19A	28.201	FC-2	sanidine	0.005400	0.000140	0.012100	0.000050	0.000000	0.000000	0.000695	0.000018	0.0000196	0.0000016	0.000265	0.000004	263.000000	2.320000	0.227000
20A	28.201	FC-2	sanidine	0.005400	0.000140	0.012100	0.000050	0.000000	0.000000	0.000695	0.000018	0.0000196	0.0000016	0.000265	0.000004	263.000000	2.320000	0.227000
21A	28.201	FC-2	sanidine	0.005400	0.000140	0.012100	0.000050	0.000000	0.000000	0.000695	0.000018	0.0000196	0.0000016	0.000265	0.000004	263.000000	2.320000	0.227000
22A	28.201	FC-2	sanidine	0.005400	0.000140	0.012100	0.000050	0.000000	0.000000	0.000695	0.000018	0.0000196	0.0000016	0.000265	0.000004	263.000000	2.320000	0.227000
23A	28.201	FC-2	sanidine	0.005400	0.000140	0.012100	0.000050	0.000000	0.000000	0.000695	0.000018	0.0000196	0.0000016	0.000265	0.000004	263.000000	2.320000	0.227000
25A	28.201	FC-2	sanidine	0.005400	0.000140	0.012100	0.000050	0.000000	0.000000	0.000695	0.000018	0.0000196	0.0000016	0.000265	0.000004	263.000000	2.320000	0.227000
X 26A	28.201	FC-2	sanidine	0.005400	0.000140	0.012100	0.000050	0.000000	0.000000	0.000695	0.000018	0.0000196	0.0000016	0.000265	0.000004	263.000000	2.320000	0.227000
27A	28.201	FC-2	sanidine	0.005400	0.000140	0.012100	0.000050	0.000000	0.000000	0.000695	0.000018	0.0000196	0.0000016	0.000265	0.000004	263.000000	2.320000	0.227000
28A	28.201	FC-2	sanidine	0.005400	0.000140	0.012100	0.000050	0.000000	0.000000	0.000695	0.000018	0.0000196	0.0000016	0.000265	0.000004	263.000000	2.320000	0.227000
29A	28.201	FC-2	sanidine	0.005400	0.000140	0.012100	0.000050	0.000000	0.000000	0.000695	0.000018	0.0000196	0.0000016	0.000265	0.000004	263.000000	2.320000	0.227000

Sample: K-07-01-C **Identifier: UW144:A8**
Material: Sanidine **Location: GSSP type locality Pubelo, Colorado, USA (bed 89 of Kennedy et al., 2005)**

N	Power %	Age (Ma)	±1σ (Ma)	K/Ca	±1σ	%^{40}Ar (%)	^{40}Ar*/^{39}Ar$_K$	Corrected[1] ^{40}Ar (cps)	±1σ	^{39}Ar (cps)	±1σ	^{38}Ar (cps)	±1σ
02A	18	93.80	0.22	67.34	12.665	98.685	3.1401914	183040.5528808	164.3509007	57461.8605233	44.0122429	690.1771642	4.218812
02A	18	94.31	0.21	48.694	6.261	98.998	3.1574677	197749.6494439	179.8350526	61935.6574239	51.1064677	747.7697027	5.2779039
03A	18	93.62	0.30	32.575	3.789	98.633	3.1339205	140010.7973566	131.3282129	44018.2779701	45.2744438	532.7891117	4.0032144
04A	18	94.34	0.27	74.389	21.158	98.892	3.1585869	145429.9887467	136.5958152	45483.7961463	42.8910278	548.4850129	3.6412074
05A	18	93.73	0.23	50.156	7.851	99.047	3.1377101	168725.183367	150.0745584	53204.3388109	45.4020491	636.4439693	4.1859153
06A	18	93.68	0.37	26.645	3.663	97.334	3.1359407	112632.6016499	111.0717682	34922.1082394	35.8905413	410.2607408	3.4565586
07A	18	94.01	0.53	44.974	13.517	97.331	3.1471905	74011.3206944	81.5773737	22864.5015945	29.6832892	279.4095061	2.9448728
08A	18	93.51	0.34	62.62	17.574	98.976	3.130065	114369.9054581	111.215614	36126.360803	37.3475547	442.4427403	3.601079
09A	18	93.99	0.29	51.426	10.311	98.551	3.146501	138504.7297275	133.0362742	43334.3781104	46.4654242	520.9027539	3.7772724
10A	18	94.11	0.42	36.131	7.436	98.59	3.1506564	96669.9504942	103.9393639	30217.6067925	32.5268864	367.196436	2.8764495
11A	18	94.07	0.23	108.007	38.967	99.103	3.1492606	167063.4030614	161.0180065	52516.4962757	48.1061327	628.8155682	3.9992566
12A	18	93.21	0.52	57.207	23.467	97.902	3.1200099	68732.8524844	110.8747783	21544.469597	32.4137111	253.2145649	2.441356
13A	18	94.02	0.32	101.777	43.333	97.333	3.1476064	134061.5006605	127.1111823	41411.4617739	37.8696665	497.9110232	4.1828687
14A	18	93.84	0.45	39.014	9.721	97.822	3.1414814	85811.5175961	94.8062673	26692.3483339	33.2023769	319.688873	2.8889781
15A	18	93.73	0.36	66.067	20.647	98.802	3.1375884	110867.1955104	112.7120454	34874.5999549	38.5350521	425.5222445	3.8785931
16A	18	94.32	0.32	185.151	129.801	97.613	3.1579058	155149.2715246	146.1195452	47903.0503446	47.1047283	572.8251317	4.1066729
17A	18	94.64	0.38	104.569	38.576	90.377	3.1691148	195733.6723673	179.0814239	55755.6858994	49.3214141	678.4092857	4.3095445
18A	18	94.01	0.26	51.375	9.081	96.031	3.1473132	261325.5111657	223.8318273	79640.5620748	55.6972639	971.7710167	5.9345465
19A	18	94.34	0.28	108.418	46.082	96.14	3.1587844	225506.752515	200.3610158	68552.3479247	52.7841801	829.2221102	4.9760295
20A	18	94.53	0.33	57.454	14.312	96.706	3.1650332	191480.5940191	164.2364868	58436.2364025	49.9290756	708.2126613	5.0166863
Weighted mean K/Ca ±2σ				**38.966**	**6.151**								
Weighted mean Age ±2σ		**94.02**	**0.15**	**n=20/20**		**MSWD=1.119**							

N	^{37}Ar (cps)	±1σ	^{36}Ar (cps)	±1σ	RunDate	Δt[3] (days)	J	±1σ	^{39}Ar Decay	^{37}Ar Decay	LambdaK
02A	18.6633914	3.5100843	7.1166484	1.272841	04/28/19 23:56	170.3594097	0.0167473	3.48313E-06	1.0010711	19.7282354	5.464E-10
02A	27.7899893	3.5730524	5.6598199	1.2732238	04/29/19 01:14	170.4137269	0.0167473	3.48313E-06	1.0010715	19.7494105	5.464E-10
03A	29.5153267	3.4330262	5.7694066	1.3731416	04/29/19 01:34	170.4276852	0.0167473	3.48313E-06	1.0010716	19.7548557	5.464E-10
04A	13.3409013	3.7943548	4.6448334	1.2649954	04/29/19 02:52	170.4818287	0.0167473	3.48313E-06	1.001072	19.7759916	5.464E-10
05A	23.1386918	3.6216732	4.5393717	1.2418265	04/29/19 03:12	170.4957523	0.0167473	3.48313E-06	1.0010721	19.7814305	5.464E-10
06A	28.5778626	3.9282241	9.5709017	1.3923004	04/29/19 03:41	170.5159491	0.0167473	3.48313E-06	1.0010722	19.7893226	5.464E-10
07A	11.0703305	3.3272441	6.2618365	1.344645	04/29/19 05:19	170.5838194	0.0167473	3.48313E-06	1.0010727	19.8158668	5.464E-10
08A	12.5589594	3.5245283	3.3361485	1.326475	04/29/19 05:39	170.5977546	0.0167473	3.48313E-06	1.0010728	19.8213213	5.464E-10
09A	18.324449	3.6739836	6.0343273	1.2939172	04/29/19 06:57	170.6519792	0.0167473	3.48313E-06	1.0010732	19.842560	5.464E-10
10A	18.1817931	3.7416528	4.114756	1.3872845	04/29/19 07:17	170.6658218	0.0167473	3.48313E-06	1.0010733	19.8479855	5.464E-10
11A	10.5664886	3.8122028	4.1205193	1.1973284	04/29/19 07:46	170.6859838	0.0167473	3.48313E-06	1.0010734	19.8558906	5.464E-10
12A	8.1818412	3.3561732	4.4806826	1.1895406	04/29/19 08:06	170.699919	0.0167473	3.48313E-06	1.0010735	19.8613561	5.464E-10
13A	8.8362213	3.7621305	11.2690689	1.4295336	04/29/19 08:36	170.7202199	0.0167473	3.48313E-06	1.0010737	19.8693209	5.464E-10
14A	14.8477982	3.6994099	5.8522977	1.3012058	04/29/19 09:25	170.7543056	0.0167473	3.48313E-06	1.0010739	19.8827013	5.464E-10
15A	11.4449781	3.5767813	3.8776244	1.343034	04/29/19 10:34	170.8022801	0.0167473	3.48313E-06	1.0010742	19.901549	5.464E-10
16A	4.5756865	3.2078039	11.5609666	1.6222166	05/09/19 18:12	181.1206944	0.0167473	3.48313E-06	1.0011473	24.4000762	5.464E-10
17A	9.4234606	3.4763061	62.1357439	2.2829724	05/09/19 19:01	181.154838	0.0167473	3.48313E-06	1.0011475	24.4165355	5.464E-10
18A	23.5127102	4.1560322	33.4748019	2.139889	05/17/19 12:54	188.8997685	0.0167473	3.48313E-06	1.0012023	28.4521283	5.464E-10
19A	9.5840286	4.0736011	27.9850389	2.0147053	05/17/19 13:43	188.9337037	0.0167473	3.48313E-06	1.0012025	28.4712039	5.464E-10
20A	15.4060678	3.8377166	20.1799891	2.0511837	05/17/19 14:32	188.9679514	0.0167473	3.48313E-06	1.0012028	28.4904681	5.464E-10

N	MonitorAge	MonitorName	MonitorMaterial	(^{40}Ar/^{39}39)$_K$	±1σ	(^{38}Ar/^{39}39)$_K$	±1σ	(^{37}Ar/^{39}39)$_K$	±1σ	(^{39}Ar/^{37}37)$_{Ca}$	±1σ	(^{38}Ar/^{37}37)$_{Ca}$	±1σ	(^{36}Ar/^{37}37)$_{Ca}$	±1σ	(^{36}Ar/^{38}38)$_{Cl}$	Ca/K	Cl/K
02A	28.201	FC-2	sanidine	0.005400	0.000140	0.012100	0.000050	0.000000	0.000000	0.000695	0.000018	0.0000196	0.0000016	0.000265	0.000004	263.000000	2.320000	0.227000
02A	28.201	FC-2	sanidine	0.005400	0.000140	0.012100	0.000050	0.000000	0.000000	0.000695	0.000018	0.0000196	0.0000016	0.000265	0.000004	263.000000	2.320000	0.227000
03A	28.201	FC-2	sanidine	0.005400	0.000140	0.012100	0.000050	0.000000	0.000000	0.000695	0.000018	0.0000196	0.0000016	0.000265	0.000004	263.000000	2.320000	0.227000
04A	28.201	FC-2	sanidine	0.005400	0.000140	0.012100	0.000050	0.000000	0.000000	0.000695	0.000018	0.0000196	0.0000016	0.000265	0.000004	263.000000	2.320000	0.227000
05A	28.201	FC-2	sanidine	0.005400	0.000140	0.012100	0.000050	0.000000	0.000000	0.000695	0.000018	0.0000196	0.0000016	0.000265	0.000004	263.000000	2.320000	0.227000
06A	28.201	FC-2	sanidine	0.005400	0.000140	0.012100	0.000050	0.000000	0.000000	0.000695	0.000018	0.0000196	0.0000016	0.000265	0.000004	263.000000	2.320000	0.227000
07A	28.201	FC-2	sanidine	0.005400	0.000140	0.012100	0.000050	0.000000	0.000000	0.000695	0.000018	0.0000196	0.0000016	0.000265	0.000004	263.000000	2.320000	0.227000
08A	28.201	FC-2	sanidine	0.005400	0.000140	0.012100	0.000050	0.000000	0.000000	0.000695	0.000018	0.0000196	0.0000016	0.000265	0.000004	263.000000	2.320000	0.227000
09A	28.201	FC-2	sanidine	0.005400	0.000140	0.012100	0.000050	0.000000	0.000000	0.000695	0.000018	0.0000196	0.0000016	0.000265	0.000004	263.000000	2.320000	0.227000
10A	28.201	FC-2	sanidine	0.005400	0.000140	0.012100	0.000050	0.000000	0.000000	0.000695	0.000018	0.0000196	0.0000016	0.000265	0.000004	263.000000	2.320000	0.227000
11A	28.201	FC-2	sanidine	0.005400	0.000140	0.012100	0.000050	0.000000	0.000000	0.000695	0.000018	0.0000196	0.0000016	0.000265	0.000004	263.000000	2.320000	0.227000
12A	28.201	FC-2	sanidine	0.005400	0.000140	0.012100	0.000050	0.000000	0.000000	0.000695	0.000018	0.0000196	0.0000016	0.000265	0.000004	263.000000	2.320000	0.227000
13A	28.201	FC-2	sanidine	0.005400	0.000140	0.012100	0.000050	0.000000	0.000000	0.000695	0.000018	0.0000196	0.0000016	0.000265	0.000004	263.000000	2.320000	0.227000
14A	28.201	FC-2	sanidine	0.005400	0.000140	0.012100	0.000050	0.000000	0.000000	0.000695	0.000018	0.0000196	0.0000016	0.000265	0.000004	263.000000	2.320000	0.227000
15A	28.201	FC-2	sanidine	0.005400	0.000140	0.012100	0.000050	0.000000	0.000000	0.000695	0.000018	0.0000196	0.0000016	0.000265	0.000004	263.000000	2.320000	0.227000
16A	28.201	FC-2	sanidine	0.005400	0.000140	0.012100	0.000050	0.000000	0.000000	0.000695	0.000018	0.0000196	0.0000016	0.000265	0.000004	263.000000	2.320000	0.227000
17A	28.201	FC-2	sanidine	0.005400	0.000140	0.012100	0.000050	0.000000	0.000000	0.000695	0.000018	0.0000196	0.0000016	0.000265	0.000004	263.000000	2.320000	0.227000
18A	28.201	FC-2	sanidine	0.005400	0.000140	0.012100	0.000050	0.000000	0.000000	0.000695	0.000018	0.0000196	0.0000016	0.000265	0.000004	263.000000	2.320000	0.227000
19A	28.201	FC-2	sanidine	0.005400	0.000140	0.012100	0.000050	0.000000	0.000000	0.000695	0.000018	0.0000196	0.0000016	0.000265	0.000004	263.000000	2.320000	0.227000
20A	28.201	FC-2	sanidine	0.005400	0.000140	0.012100	0.000050	0.000000	0.000000	0.000695	0.000018	0.0000196	0.0000016	0.000265	0.000004	263.000000	2.320000	0.227000

Notes:

[1]Corrected: Isotopic intensities corrected for blank, baseline, radioactivity decay and detector intercalibration, not for interfering reactions.

[3]Time interval (days) between end of irradiation and beginning of analysis.

X symbol preceding sample ID denotes analyses excluded from weighted-mean age calculations.

Errors quoted for individual analyses include analytical error only, without interfering reaction or J uncertainties.

Decay constants and isotopic abundances after Min et al. (2000)

Ages calculated relative to FCS-2 Fish Canyon sanidine interlaboratory standard at 28.201 Ma (Kuiper et al. 2008)

Supplemental References

Barker, I. R., Moser, D. E., Kamo, S. L., and Plint, A. G., 2011, High-precision U–Pb zircon ID–TIMS dating of two regionally extensive bentonites: Cenomanian Stage, Western Canada Foreland Basin: Canadian Journal of Earth Sciences, v. 48, no. 2, p. 543-556, https://doi.org/10.1139/E10-042.

Brett, C. E., 1995, Sequence stratigraphy, biostratigraphy, and taphonomy in shallow marine environments: Palaois, v. 10, p. 597-616, https://doi.org/ 10.2307/3515097.

Cobban, W. A., and Scott, G. R., 1972, Stratigraphy and ammonite fauna of the Graneros Shale and Greenhorn Limestone near Pueblo, Colorado: U.S. Geological Survey Professional Paper 645, 108 p., https://doi.org/10.3133/pp645.

Du Vivier, A. D. C., Selby, D., Sageman, B. B., Jarvis, I., Groecke, D. R., and Voigt, S., 2014, Marine Os-187/Os-188 isotope stratigraphy reveals the interaction of volcanism and ocean circulation during Oceanic Anoxic Event 2: Earth and Planetary Science Letters, v. 389, p. 23-33, http://dx.doi.org/10.1016/j.epsl.2013.12.024.

Eicher, D. L., and Diner, R., 1989, Origin of the cretaceous bridge creek cycles in the western interior, United States: Palaeogeography, Palaeoclimatology, Palaeoecology, v. 74, no. 1, p. 127-146, https://doi.org/10.1016/0031-0182(89)90023-0.

Elder, W. P., 1988, Geometry of Upper Cretaceous bentonite beds: Implications about volcanic source areas and paleowind patterns, western interior, United States: Geology, v. 16, no. 9, p. 835-838, https://doi.org/10.1130/0091-7613(1988)016%3C0835:GOUCBB%3E2.3.CO;2.

Elder, W. P., 1989, Molluscan extinction patterns across the Cenomanian-Turonian Stage boundary in the Western Interior of the United States: Paleobiology, v. 15, no. 3, p. 299-320, https://doi.org/10.1017/S0094837300009465.

Elder, W. P., Gustason, E. R., and Sageman, B. B., 1994, Correlation of basinal carbonate cycles to nearshore parasequences in the Late Cretaceous Greenhorn seaway, Western Interior U.S.A: Geological Society of America Bulletin, v. 106, no. 7, p. 892-902, https://doi.org/10.1130/0016-7606(1994)106%3C0892:COBCCT%3E2.3.CO;2.

Elder, W. P., and Kirkland, J. I., 1985, Stratigraphy and Depositional Environments of the Bridge Creek Limestone Member of the Greenhorn Limestone at Rock Canyon Anticline Near Pueblo, Colorado, *in* Pratt, L. M., Kauffman, E. G., and Zelt, F. B., eds., Fine-Grained Deposits and Biofacies of the Cretaceous Western Interior Seaway: Evidence of Cyclic Sedimentary Processes, SEPM Society for Sedimentary Geology, p.122-134, https://doi.org/10.2110/sepmfg.04.122.

Eldrett, J. S., Ma, C., Bergman, S. C., Lutz, B., Gregory, F. J., Dodsworth, P., Phipps, M., Hardas, P., Minisini, D., Ozkan, A., Ramezani, J., Bowring, S. A., Kamo, S. L., Ferguson, K., Macaulay, C., and Kelly, A. E., 2015, An astronomically calibrated stratigraphy of the Cenomanian, Turonian and earliest Coniacian from the Cretaceous Western Interior Seaway, USA: Implications for global chronostratigraphy: Cretaceous Research, v. 56, p. 316-344, https://doi.org/10.1016/j.cretres.2015.04.010.

Kennedy, W.J., Walaszczyk, I., and Cobban, W.A., 2000, Pueblo, Colorado, USA, candidate Global Boundary Stratotype Section and Point for the base of the Turonian Stage of the Cretaceous, and for the base of the Middle Turonian Substage, with a revision of the *Inoceramidae* (Bivalvia): Acta Geologica Polonica, v. 50, no. 3, p. 295–334.

Kennedy, W. J., Walaszczyk, I., and Cobban, W. A., 2005, The global boundary stratotype section and point for the base of the Turonian stage of the cretaceous: Pueblo, Colorado, USA: Episodes, v. 28, no. 2, p. 93-104.

Kirkland, J.I., 1991, Lithostratigraphic and biostratigraphic framework for the Mancos Shale (Late Cenomanian to Middle Turonian) at Black Mesa, northeastern Arizona, *in* Nations, J.D., and Eaton, J.G., eds., Stratigraphy, Depositional Environments, and Sedimentary Tectonics of the Western Margin, Cretaceous Western Interior Seaway: Geological Society of America Special Paper 260, p. 85–111, https://doi.org/10.1130/SPE260-p85.

Jicha, B. R., Singer, B. S., and Sobol, P., 2016, Re-evaluation of the ages of 40Ar/39Ar sanidine standards and supereruptions in the western U.S. using a Noblesse multi-collector mass spectrometer: Chemical Geology, v. 431, p. 54-66, https://doi.org/10.1016/j.chemgeo.2016.03.024.

Jicha, B. R., and Brown, F. H., 2014, An age for the Korath Range, Ethiopia and the viability of 40Ar/39Ar dating of kaersutite in Late Pleistocene volcanics: Quaternary Geochronology, v. 21, p. 53-57 https://doi.org/10.1016/j.quageo.2013.03.007.

Jones, M. M., Sageman, B. B., Oakes, R. L., Parker, A. L., Leckie, R. M., Bralower, T. J., Sepúlveda, J., and Fortiz, V., 2019, Astronomical pacing of relative sea level during Oceanic Anoxic Event 2: Preliminary studies of the expanded SH#1 Core, Utah, USA: GSA Bulletin, v. 131, no. 9-10, p. 1702-1722, https://doi.org/10.1130/B32057.1.

Joo, Y. J., and Sageman, B. B., 2014, Cenomanian to Campanian carbon isotope chemostratigraphy from the Western Interior Basin, USA: Journal of Sedimentary Research, v. 84, no. 7, p. 529-542, https://doi.org/10.2110/jsr.2014.38.

Kuiper, K. F., Deino, A., Hilgen, F. J., Krijgsman, W., Renne, P. R., and Wijbrans, J. R., 2008, Synchronizing Rock Clocks of Earth History: Science, v. 320, no. 5875, p. 500-504, DOI: 10.1126/science.1154339.

Laurin, J., Barclay, R. S., Sageman, B. B., Dawson, R. R., Pagani, M., Schmitz, M., Eaton, J., McInerney, F. A., and McElwain, J. C., 2019, Terrestrial and marginal-marine record of the mid-Cretaceous Oceanic Anoxic Event 2 (OAE 2): High-resolution framework, carbon isotopes, CO2 and sea-level change: Palaeogeography, Palaeoclimatology, Palaeoecology, v. 524, p. 118-136, https://doi.org/10.1016/j.palaeo.2019.03.019.

Lee, J., Marti, K., Severinghaus, J. P., Kawamura, K., Yoo, H., Lee, J. B., Kim, J. S., 2006, A redetermination of the isotopic abundances of atmospheric Ar: Geochimica et Cosmochimica Acta, v. 70, no. 17, p. 4507-4512, https://doi.org/10.1016/j.gca.2006.06.1563.

Ma, C., Meyers, S. R., Sageman, B. B., Singer, B. S., and Jicha, B. R., 2014, Testing the astronomical time scale for oceanic anoxic event 2, and its extension into Cenomanian strata of the Western Interior Basin (USA): Geological Society of America Bulletin, v. 126, no. 7-8, p. 974-989, https://doi.org/10.1130/B30922.1.

Meyers, S.R., Sageman, B.B., and Hinnov, L.A., 2001, Integrated quantitative stratigraphy of the Cenomanian- Turonian Bridge Creek Limestone member using evolutive harmonic analysis and stratigraphic modeling: Journal of Sedimentary Research, v. 71, no. 4, p. 628–644, https://doi.org/10.1306/012401710628.

Meyers, S. R., and Sageman, B. B., 2004, Detection, quantification, and significance of hiatuses in pelagic and hemipelagic strata: Earth and Planetary Science Letters, v. 224, no. 1-2, p. 55-72, https://doi.org/10.1016/j.epsl.2004.05.003.

Meyers, S. R., Siewert, S. E., Singer, B. S., Sageman, B. B., Condon, D. J., Obradovich, J. D., Jicha, B. R., and Sawyer, D. A., 2012b, Intercalibration of radioisotopic and astrochronologic time scales for the Cenomanian-Turonian boundary interval, Western Interior Basin, USA: Geology, v. 40, no. 1, p. 7-10, https://doi.org/10.1130/G32261.1.

Min, K., Mundil, R., Renne, P. R., and Ludwig, K. R., 2000, A test for systematic errors in 40Ar/39Ar geochronology through comparison with U/Pb analysis of a 1.1-Ga rhyolite: Geochimica et Cosmochimica Acta, v. 64, no. 1, p. 73-98, https://doi.org/10.1016/S0016-7037(99)00204-5.

Pratt, L. M., 1984, Influence of paleoenvironmental factors on preservation of organic matter in Middle Cretaceous Greenhorn Formation, Pueblo, Colorado: AAPG Bulletin, v. 68, no. 9, p. 1146-1159, https://doi.org/10.1306/AD4616E7-16F7-11D7-8645000102C1865D.

Renne, P. R., Sharp, Z. D., Heizler, M. T., 2008, Cl-derived argon isotope production in the CLICIT facility of OSTR reactor and the effects of the Cl-correction in 40Ar/39Ar geochronology, Chemical Geology, v. 255, no. 3-4, p. 463-466, https://doi.org/10.1016/j.chemgeo.2008.07.014.

Sageman, B. B., Meyers, S. R., and Arthur, M. A., 2006, Orbital time scale and new C-isotope record for Cenomanian-Turonian boundary stratotype: Geology, v. 34, no. 2, p. 125-128, https://doi.org/10.1130/G22074.1.

Sageman, B. B., Singer, B. S., Meyers, S. R., Siewert, S. E., Walaszczyk, I., Condon, D. J., Jicha, B. R., Obradovich, J. D., and Sawyer, D. A., 2014b, Integrating Ar-40/Ar-39, U-Pb, and astronomical clocks in the Cretaceous Niobrara Formation, Western Interior Basin, USA: Geological Society of America Bulletin, v. 126, no. 7-8, p. 956-973, https://doi.org/10.1130/B30929.1.

Sullivan, D. L., Brandon, A. D., Eldrett, J., Bergman, Minisini, D., S. C., Wright, S. (in press) High Resolution Osmium Data Record Three Distinct Pulses of Magmatic Activity During Cretaceous Ocean Anoxic Event 2 (OAE 2): Geochimica et Cosmochimica Acta, https://doi.org/10.1016/j.gca.2020.04.002.

Tibert, N. E., Leckie, R. M., Eaton, J. G., Kirkland, J. I., Colin, J.-P., Leithold, E. L., and McCormic, M. E., 2003, Recognition of relative sea-level change in Upper Cretaceous coal-bearing strata: a paleoecological approach using agglutinated foraminifera and ostracodes to detect key stratigraphic surfaces, *in* C, O. H., and Leckie, R. M., eds., Micropaleontologic proxies for sea-level change and stratigraphic discontinuities, Volume 75, Society for Sedimentary Geology, p. 263-299, https://doi.org/10.2110/pec.03.75.0263.

Uličný, D., 1999, Sequence stratigraphy of the Dakota Formation (Cenomanian), southern Utah: interplay of eustasy and tectonics in a foreland basin: Sedimentology, v. 46, no. 5, p. 807-836, https://doi.org/10.1046/j.1365-3091.1999.00252.x.